Cellular Physiology and Biochemistry

Cell Physiol Biochem 2022;56:663-684
DOI: 10.33594/000000589
Published online: 25 November 2022
Accepted: 8 November 2022







**Review**

# The Special One: Architecture, Physiology and Pharmacology of the TRESK Channel

Julian A. Schreiber[a,b] Martina Düfer[b] Guiscard Seebohm[a]

[a]University Hospital Münster, Institute for Genetics of Heart Diseases (IfGH), Department of Cardiovascular Medicine, Münster, Germany, [b]University of Münster, Institute of Pharmaceutical and Medicinal Chemistry, Department of Pharmacology, Münster, Germany

**Key Words**
$K_{2P}$ channels • TRESK • Pharmacology • Ion channel • Pain • Epilepsy

**Abstract**
The TWIK-related spinal cord $K^+$ channel (TRESK) is part of the two-pore domain $K^+$ channel family ($K_{2P}$), which are also called leak potassium channels. As indicated by the channel family name, TRESK conducts $K^+$ ions along the concentration gradient in a nearly voltage-independent manner leading to lowered membrane potentials. Although functional and pharmacological similarities exist, TRESK shows low sequence identity with other $K_{2P}$ channels. Moreover, the channel possesses several unique features such as its sensitivity to intracellular $Ca^{2+}$ ions, that are not found in other $K_{2P}$ channels. High expression rates are found in immune-associated and neuronal cells, especially in sensory neurons of the dorsal root and trigeminal ganglia. As a consequence of the induced hyperpolarization, TRESK influences neuronal firing, the release of inflammatory mediators and the proliferation of distinct immune cells. Consequently, this channel might be a suitable target for pharmacological intervention in migraine, epilepsy, neuropathic pain or distinct immune diseases. In this review, we summarize the biochemical and biophysical properties of TRESK channels as well as their sensitivity to different known compounds. Furthermore, we give a structured overview about the physiological and pathophysiological impact of TRESK, that render the channel as an interesting target for specific drug development.



## Introduction – The $K_{2P}$ Channel Family

Potassium ($K^+$) ion channels are essential for the viability and electrical integrity of nearly all living cells [1]. As a result of selective $K^+$ permeation along the concentration gradient they are crucial for the maintenance of membrane potential as well as repolarization [2, 3]. With more than 80 different genes encoding channel-forming subunits (α subunits) $K^+$ channels represent the most diverse group of selective ion channels [4]. So far, four different families are known: voltage-gated ($K_v$), inward rectifying ($K_{ir}$), $Ca^{2+}$- or $Na^+$-activated ($K_{Ca}$ / $K_{Na}$), and two pore domain $K^+$ channels ($K_{2P}$) [5].

Dr. Julian Alexander Schreiber
Institute for Genetics of Heart Diseases (IfGH), Department of Cardiovascular Medicine, University Hospital Münster, Robert-Koch-Straße 45, D-48149 Münster (Germany)
Tel. +49-251-835872, E-Mail j.schreiber@uni-muenster.de

The first member of the mammalian $K_{2P}$ channel family was identified in 1996 [6]. Surprisingly, it shows a novel channel architecture completely different to the other known mammalian $K^+$ channels (Fig. 1A-1C) [6]. While $K_v$-, $K_{ir}$ and $K_{Ca}$ / $K_{Na}$ assemble as tetramers of α subunits, this channel has a homodimeric structure [6]. On the other hand, each monomer possesses two instead of one pore forming region, each comprised of the pore helix (P1/P2) and the pore loop (SF1/SF2) (Fig. 1A, 1C) [6]. Consequently, assembling of two monomers results in the formation of a tetramer-like selectivity filter (SF), that is similar to the SF of other $K^+$ channels ensuring the selective permeation of $K^+$ ions [7]. Heterologous expression of the channel results in an almost linear current-voltage relationship with a weak inward rectification [6]. Therefore, it was named TWIK1, which stands for "tandem of pore domains in a weak inward rectifying $K^+$ channel 1" [6].

Today, 15 different genes encoding $K_{2P}$ subunits are known, that commonly form homodimers [8]. Recent studies suggest, that heterodimerization can occur for some $K_{2P}$ subunits, which is comprehensible due to their highly related monomer structure [9–12]. Beside the typical pair of pore-forming regions (P1/P2, SF1/SF2) each monomer possesses four transmembrane helices (M1-M4) and two extracellular helices (C1, C2) (Fig. 1A-1C) [13]. In the dimeric channel, C1 and C2 form the typical Cap-structure, that is responsible for the insensitivity of $K_{2P}$ channels to most classical $K^+$ channel pore blockers and peptide toxins [13, 14]. Interestingly, many $K_{2P}$ channels have an extended intracellular C-terminus, that is involved in functional modulation of the ion channel by phospholipids, fatty acids, and regulatory proteins [15, 16].

Since $K_{2P}$ channels adopt conductive states over a broad range of voltages, they are also called $K^+$ leak channels [17]. However, their open probability can be effectively modulated by different entities like membrane tension, $H^+$, phosphatidylinositol 4,5-bisphosphate ($PIP_2$), volatile anesthetics or temperature [18]. Contrary to $K_v$ channels, most $K_{2P}$ channels do not possess an intracellular gate [18]. Therefore, the gating process is mainly controlled by the SF, that shows a behavior similar to C-type inactivation of $K_v$ channels [19–22]. However, recent studies identified the X gate at TASK channels, that is located at the inner vestibule controlling the pharmacodynamics of TASK-1 channel inhibitors [23].

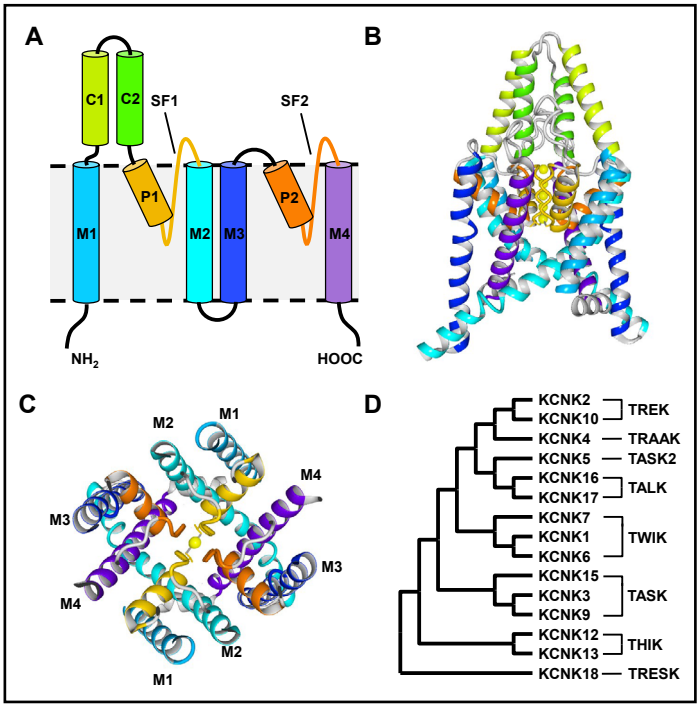


**Fig. 1.** A. Secondary structure of $K_{2P}$ channel monomer. Cap-domain is formed by helices C1/C2 (green), while helices M1-M4 (blue, purple), pore helices (P1/P2) and loops (SF1/SF2) form the ion pore. B. Cryo-EM structure of homodimeric TWIK1 channel (PDB 7SK0). Color-code is defined in A. C. Top view of TWIK1 channel without Cap-domain. Color code is defined in A. Selectivity filter is formed by P1/SF1 and P2/SF2 while lower ion pathway is formed by inner helices M2 and M4. D. Phylogenetic tree of KCNK1-18 protein sequences. Tree was assembled using MEGA X [122] and protein sequences from accession numbers NP002236.1 (KCNK1), NP001017424.1 (KCNK2), NP002237.1 (KCNK3), NP201567.1 (KCNK4), NP003737.1 (KCNK5) NP004814.1 (KCNK6), NP005705.1 (KCNK7), NP001269463.1 (KCNK9), NP201567.1 (KCNK10), AAG32313.1 (KCNK12), ACH86101.1 (KCNK13), NP071753.2 (KCNK15), NP001128577.1 (KCNK16), NP113648.2 (KCNK17) and NP862823.1 (KCNK18).

Based on their functional properties $K_{2P}$ channels can be subdivided into subfamilies of weakly inward rectifying (TWIK), TWIK-related (TREK), acid-sensitive (TASK), arachidonic acid-sensitive (TRAAK), alkaline-activated (TALK), halothane-inhibited (THIK) and TWIK-related spinal cord (TRESK) $K^+$ channels (Fig. 1D) [24]. The last identified $K_{2P}$ channel is TRESK, which was found in 2003 by analysis of the human genome data base [25]. Although structural similarity is assumed, sequence identity compared to the other $K_{2P}$ channels is only 13 - 19 % [25]. Low sequence identity as well as several unique features render TRESK as the most diverse channel of the $K_{2P}$ family. The structural, biophysical, and pharmacological properties of TRESK are explained in the following paragraphs of this review. Furthermore, the significance of TRESK channels for physiological and pathophysiological processes is discussed in detail.

## Protein sequence differences of TRESK

Comparing the protein sequences identifies TRESK as the most divergent $K_{2P}$ channel. Alignment of human TWIK1 with human (h), mice (m) and rat (r) TRESK results in a sequence identity of approximately 20 % (Fig. 2). A major reason for this low sequence identity is the intracellular loop formed by more than 100 amino acids between M2 and M3 representing a functional domain, that is absent in all other $K_{2P}$ channels (Fig. 2, Fig. 3A-3B) [25]. This domain is responsible for the unique sensitivity of TRESK to cytosolic $Ca^{2+}$ ions, which increase channel activity via a mechanism that includes calcineurin binding to the M2/M3 loop and subsequent channel dephosphorylation [25, 26]. Further, TRESK does not possess an extended C-terminus, which enables the interaction of $K_{2P}$ channels with regulatory proteins [15, 16].

Since many species differences are described in literature, we specified the species for properties of the mouse (m), rat (r), zebrafish (z) and human (h) channel orthologues, that are different or not directly transferable for other TRESK orthologues. The protein sequence of mTRESK, which was isolated in 2004 from testis show moderate sequence identity as well [27]. Due to only 65 % identity compared to hTRESK, it was speculated that the identified channel could be a new member of the TRESK subfamily [27]. Consequently, it was named TRESK2 [27]. However, until today no second TRESK channel has been identified, neither in mouse nor in human.

Protein sequences of other species show comparable (rat) or even lower (zebrafish) sequence identity leading to increased possibility of species-dependent biophysical, physiological or pharmacological properties [28]. For example, the zebrafish orthologue shares only 32 % identity with hTRESK, but exerts similar behavior regarding the overall biophysical properties [28]. However, zTRESK cannot be inhibited by the hTRESK inhibitor quinidine and shows no sensitivity to increased cytosolic $Ca^{2+}$ levels, since it does not possess the calcineurin binding motif at the M2/M3 loop [28].

## Biophysical properties and endogenous modulation

Expression of hTRESK in *Xenopus laevis* oocytes generates outward rectifying currents in the whole cell configuration, that are depending on the extracellular $K^+$ concentration [25]. Channel function is not influenced by temperature, but similar to other $K_{2P}$ channels, sensitivity to membrane stretch or changes in osmolarity is detected in experiments using rTRESK [25, 29]. Membrane tension by shear stress as well as hypotonicity increase channel open probability, while hypertonicity results in channel inhibition [29]. Single channel recordings of mTRESK show different behavior depending on current direction even under symmetrical $K^+$ conditions with a conductance ranging from 12 pS (outward) to 16 pS (inward) [27, 30]. Outward currents are characterized by robust square shaped openings while inward currents appear as very short burst like openings [27, 30].

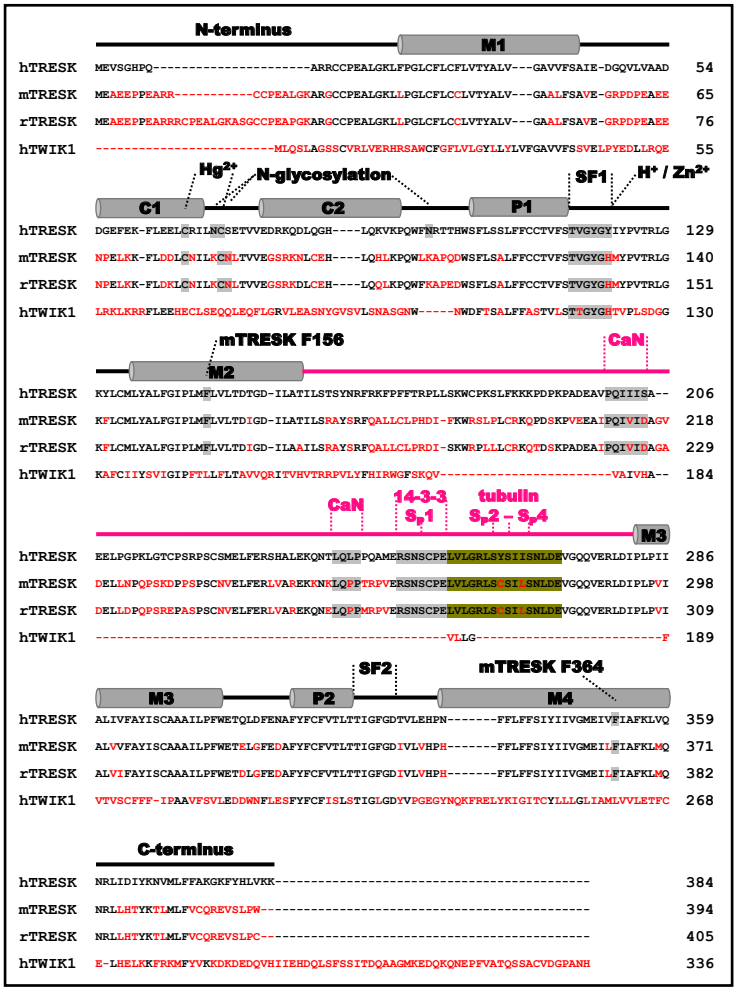


**Fig. 2.** Protein sequence alignment of hTRESK (NP_862823.1), mTRESK (NP_997144), rTRESK (NP_001003820.1) and hTWIK1 (NP_002236.1). Secondary structure elements (M1-M4, C1/C2, P1/P2) based on Sano et al. [25] are given for hTRESK. Amino acids identical with hTRESK are colored black, while non-conserved residues are red. M2/M3 loop is indicated by magenta line. Important residues for selectivity filter loop (SF1, SF2), $Hg^{2+}/H^{+}/Zn^{2+}$ binding as well as binding motifs for calcineurin (CaN) and 14-3-3 adapter proteins are highlighted in gray or olive (tubulin, $S_P2$-$S_P4$).

Similar to most other $K_{2P}$ channels experimental data suggest, that TRESK gating is not influenced by bundle crossing at the intracellular site [31]. Application of $Ba^{2+}$ ions to the intracellular site in excised inside-out membrane patches results in channel inhibition [31]. The kinetics of TRESK channel inhibition by $Ba^{2+}$ is independent from the channel activity as well as the phosphorylation state of TRESK [31]. This indicates that channel activity is not controlled by an intracellular gate with flexible diameter [31]. On the other hand, mutation of residues from M2 or M4 that form the inner cavity beneath the SF can influence the channel activity. Mutation of mTRESK F154 (M2) and F364 (M4) to alanine result in strongly increased channel activity (Fig. 3C) [32]. Furthermore, the double mutant mTRESK F154A/F364A is insensitive to the $Ca^{2+}$ mobilizing compound ionomycin as well as the known TRESK channel activator cloxyquin rendering this double mutant as constitutively active [32].

Contrary to rodent TRESK channels, the human orthologue is not sensitive to extracellular pH alterations [33]. $H^{+}$ sensitivity is generated by a histidine (mTRESK H132, rTRESK H143) at the extracellular end of the SF, that is also present in other $K_{2P}$ channels but replaced with a tyrosine in hTRESK deleting $H^{+}$ sensitivity (Fig. 3C) [33–35]. At pH 5 mTRESK currents are inhibited by around 50 %, while pH >8 leads to current elevation [33]. $H^{+}$ sensitivity can be generated by replacing the hTRESK tyrosine with a histidine (hTRESK Y121H) [33]. Recent cryo-EM studies using TWIK1 indicate, that inhibition by low pH is generated by an upward movement of the histidine, subsequently destabilizing the SF [7]. Furthermore, this histidine is responsible for binding of $Zn^{2+}$ ions generating similar species-dependent inhibitory sensitivity to these ions as well [36].

Contrary to $H^+$ / $Zn^{2+}$, $Hg^{2+}$ ions are able to inhibit mTRESK and hTRESK channels suggesting a different binding site [36]. Due to the non-reversible inhibition, it was speculated that the mechanism is based on the formation of $Hg^{2+}$-thiolate complexes with cysteines [36]. Mutational analyses identified two extracellular cysteines (mTRESK C77, C82) at the Cap-structure that might be involved into $Hg^{2+}$ binding (Fig. 3C) [36]. However, double mutant mTRESK C77S/C82S cannot abolish $Hg^{2+}$ inhibition completely [36]. Since other $K_{2P}$ channels are not inhibited or even activated by $Hg^{2+}$ ions, they might be useful for pharmacological differentiation *in vitro*, but toxicological and reactivity aspects limit the usage [36].

The Cap-structure also influences the surface expression and / or trafficking of mTRESK and hTRESK via *N*-glycosylation [37]. Within the first identification of hTRESK the authors identified two possible asparagine residues suitable for *N*-glycosylation [25]. hTRESK N70 as well as the corresponding mTRESK N83 are located at the top of the Cap-structure (Fig. 3C), while the hTRESK specific residue N96 (Fig. 2) is positioned near the extracellular site of the SF [25, 37]. Interestingly, the asparagine in the Cap-structure is neighbored by cysteine that is responsible for $Hg^{2+}$ binding (Fig. 2, Fig. 3C) [36, 37]. TEVC measurements using glycosylation-deficient mutants hTRESK N70Q and N96Q as well as the corresponding double mutant reveal significant current reduction between 20-60 % compared to wildtype channels (WT) [37]. For the mTRESK mutant N83Q even a higher current reduction of 80 % compared to the WT is observed [37]. Mobility shift assays confirm *N*-glycan formation for hTRESK N70 and mTRESK N83 by comparison to the corresponding mutants [37]. For single hTRESK N96Q mutation no mobility shift compared to WT can be detected indicating a dominant role of N70 [37]. Nevertheless, reduced currents for all mutants correlate with a significant lower surface expression [37].

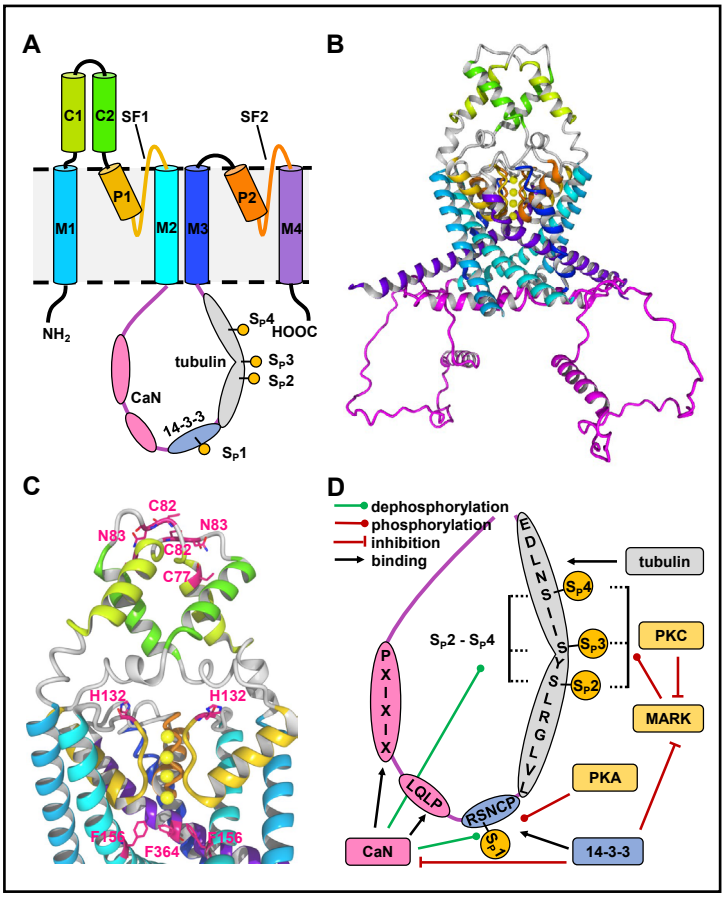


**Fig. 3.** A. Schematic depiction of TRESK monomers including M2/M3 loop (magenta) with calcineurin (CaN, pink), 14-3-3 (blue) and tubulin (grey) binding sites. Phosphorylation sites $S_p1$ – $S_p4$ are indicated by yellow dots. B. Homology model of mTRESK based on KCNK18 AlphaFold structure (Uniprot Q7Z418) [123,124]. The model was generated using YASARA structure [125]. Color code is defined in panel A. C. Depiction of important amino acids (pink) at mTRESK. D. Binding motifs at the M2/M3 loop (magenta) and functional regulation of TRESK by calcineurin (CaN; pink), 14-3-3 (blue), protein kinase A and C (PKA / PKC; yellow), microtubule affinity-regulating kinases (MARK; yellow) and tubulin (grey).

TRESK channel activity can be modulated by endogenous anionic lipids and fatty acids as well [15, 25, 38]. hTRESK is strongly inhibited by arachidonic acid with an $IC_{50}$ value of 6.6 µM [25]. Partial channel inhibition can be observed for 20 µM unsaturated docosahexaenoic (DOA), linoleic (LA) and oleic acid (OA) [25]. Slightly increased inhibition is observed for 10 µM oleoyl coenzyme A (Oleoyl CoA) leading to 50-75 % inhibition of hTRESK currents [15]. Saturated fatty acids like palmitic and stearic acid do not alter hTRESK channel activity [25]. In contrast to modulation by fatty acids, channel modulation by $PIP_2$ is still debatable. Initial studies suggest that $PIP_2$ binds to the intracellular M2/M3 loop and leads to increment of channel activity. Current potentiation was only found for hTRESK rendering activation by $PIP_2$ as another species-specific property [38]. However, more recent studies could not confirm the activation of hTRESK by $PIP_2$ [15].

### Regulation of TRESK channel activity by intracellular proteins

Since the C-terminus of TRESK channels is shorter compared to other $K_{2P}$ channels, less sensitivity to regulatory proteins might be expected. However, TRESK is strongly regulated by many different proteins through interactions with distinct sections of the intracellular M2/M3 loop including the calcineurin-depending sensitivity to cytosolic $Ca^{2+}$ ions (Fig. 3) [30]. Heterologous expression of mTRESK in *Xenopus laevis* oocytes produces robust $K^+$ currents, that are elevated 5-15 times after application or injection of $Ca^{2+}$-mobilizing agents like ionomycin or inositol 1,4,5-trisphosphate ($IP_3$) [30]. In accordance with these results, injection of EGTA results in current reduction [30]. However, application of $Ca^{2+}$ to inside-out patches do not influence channel function indicating an indirect modulation of channel activity [30]. Further evidence for indirect modulation is provided by the effect of the potent calcineurin inhibitor cyclosporin A, that is able to neutralize the $Ca^{2+}$-mediated channel activation [30]. Calcineurin is a $Ca^{2+}$/calmodulin-dependent phosphatase, that binds to the NFAT-like (nuclear factor of activated T cells) binding motif (PXIXIX) located at the M2/M3 loop (Fig. 3D) [28, 39]. The PXIXIX motif is conserved in the human (PQIIIS) as well as in rat and mice sequences (both PQIVID) [28, 39]. Binding of calcineurin dephosphorylates a conserved serine ($S_p1$; hTRESK S252, mTRESK S264, rTRESK S275), that is phosphorylated under resting conditions leading to increased channel activity [26, 30, 39]. Further examination identified three more serine residues ($S_p2$-$S_p4$), that are also phosphorylated in the resting state and putatively contribute to $Ca^{2+}$- / calcineurin-induced activation ($S_p2$: hS262, mS274, rS285; $S_p3$: hS264, mS276, rS287; $S_p4$: hS269, mS279, rS290) (Fig. 3D) [40].

Interestingly, mutational analyses revealed another species-specific difference for channel regulation by calcineurin [30, 39]. While exchange of PQIVID to PQAVAD in mTRESK abolishes the calcineurin effect completely, replacement of PQIIIS with PQAAAS in hTRESK results in a channel that still possesses residual sensitivity to calcineurin [26, 39]. This behavior is explained by a second binding motif (LQLP) near $S_p1$ that facilitates calcineurin positioning for dephosphorylation at $S_p1$-$S_p4$ [39]. Only simultaneous mutation of both motifs allows to completely abrogate the effect [39].

Channel activity is also altered by 14-3-3 proteins, that bind to the RSNSCP motif at the M2/M3 loop, that is conserved in mouse and human and includes $S_p1$ (underlined) [41]. 14-3-3 proteins are dimeric adapter proteins with seven different isoforms (β, ε, η, γ, τ, ζ, and σ) known in mammals regulating different cell signaling processes by binding to phosphorylated serine/threonine in target proteins like kinases, phosphatases, receptors or ion channels [42]. Isoforms γ and η are able to modulate mTRESK activity in *Xenopus laevis*, while other isoforms show no significant effect [41]. Furthermore, isoforms ε and ζ can interact with the corresponding binding site at hTRESK [43]. The mechanism of channel modulation based on two individual pathways (Fig. 3D) [40]. For binding of 14-3-3, $S_p1$ needs to be phosphorylated [41]. Consequently, 14-3-3 competes with the activating effect of $Ca^{2+}$ / calcineurin by $S_p1$ dephosphorylation leading to reduced channel activation [40, 41]. On the other hand, a decelerated recovery after activation by $Ca^{2+}$ can be observed indicating

an aggravated transition to the phosphorylated state [40, 41]. This phenomenon can be explained by the inhibitory effect of 14-3-3 proteins on microtubule affinity-regulating kinases (MARK), that are known for regulatory effects on microtubule dynamics in neurons [44, 45]. Together with protein kinase A (PKA), these kinases are responsible for specific (re)phosphorylation of $S_p1$-$S_p4$ (Fig. 3D) [40, 41, 45]. While PKA only phosphorylates $S_p1$ but not $S_p2$-$S_p4$, MARK1-3 exclusively phosphorylate $S_p2$-$S_p4$ but not $S_p1$ [45]. In both cases, (re) phosphorylation leads to inhibition of channel function [40, 41, 45].

The specificity of regulation by MARK-mediated phosphorylation raised the question if the microtubule cytoskeleton is involved in channel regulation [43]. Indeed, evaluation by affinity chromatography and pull-down assays could verify an interaction between tubulin and the M2/M3 loop of mTRESK [43]. The binding motif was narrowed down to a 16 amino acid sequence (mTRESK $^{268}$LVLGRL<u>S</u>Y<u>S</u>II<u>S</u>NLDE$^{283}$), that encompasses the phosphorylation sites $S_p2$-$S_p4$ (underlined) (Fig. 3D) [43]. The motif is well conserved in mammals but not in birds or fishes explaining the failure of pull down with partial sequences from chicken or zebrafish [43]. Furthermore, experimental data suggest a binding competition with 14-3-3 proteins at TRESK [43]. Nevertheless, exact modulation of the channel protein by tubulin is not completely understood and further research is needed [43].

While channel inhibition by PKA can be explained by the direct phosphorylation of $S_p1$, the species-specific influence of protein kinase C (PKC) on hTRESK is more complicated [46]. Stimulation of PKC by the known activator phorbol 12-myristate-13-acetate (PMA) leads to hTRESK activation, that is reversible by application of specific PKC inhibitors [46]. However, mutational analysis of 8 possible phosphorylation sites at the M2/M3 loop of hTRESK fail to identify a direct interaction arguing for an indirect mechanism [46]. Very recently, it was shown that hTRESK activation is caused specifically by novel-type PKCη and PKCε [47]. Both isoforms decelerate (re)phosphorylation of $S_p2$-$S_p4$ by inhibition of MARK1-3 leading to prolonged presence of the dephosphorylated state subsequently increasing channel activity by a similar mechanism previously described for 14-3-3 proteins (Fig. 3D) [47].

### Expression pattern and physiological relevance of TRESK

Initial study suggested exclusive expression of the channel in the spinal cord since RT-PCR analysis of 23 different tissues failed to detect TRESK [25]. However, shortly afterwards this statement was falsified by further RT-PCR, blotting and immunohistochemical analysis, that detected TRESK in spleen, thymus, testis, pancreas, and kidney as well as in neuronal tissues like cortex, cerebellum, dorsal root (DRG) and trigeminal ganglia (TG) [27, 33, 35, 48–52]. Transcript levels in cortex, cerebellum, DRG and TG were approximately 4-6 times higher than in the spinal cord [33, 35, 50]. Moreover, extensive RNA sequencing identified TRESK as the most specific $K^+$ channel in TG [53].

The physiological role of TRESK is analyzed by several knockdown and knockout studies in mice. Functional knockout by the mutation mTRESK G339R (located in SF2) results in distinct alterations of primary cultured DRG neurons [33]. Compared to WT, DRG neurons with channels carrying the mTRESK G339R mutation are more sensitive to depolarizing stimuli resulting in increased excitability (Fig. 4A) [33]. Consistent with these observations, further knockout studies observe increased numbers of action potentials (APs) and significant lowered rheobase compared to WT [54–56]. Unexpectedly, functional as well as complete knockout of TRESK does not alter resting membrane potential [33, 54–57]. It is assumed that these observations correlate with a compensatory upregulation of other $K_{2P}$ channels like TREK-1 or TREK-2 channels, which also contribute to the background $K^+$ current in these cells [33, 54, 55]. Especially TREK-2 was previously described to generate major background $K^+$ current together with TRESK [49]. Furthermore, a recent study suggests, that TRESK possesses the ability to form functional heterodimers with TREK-1 and TREK-2 producing $K_{2P}$ channels with mixed biophysical properties derived from both channel forming subunits [11].

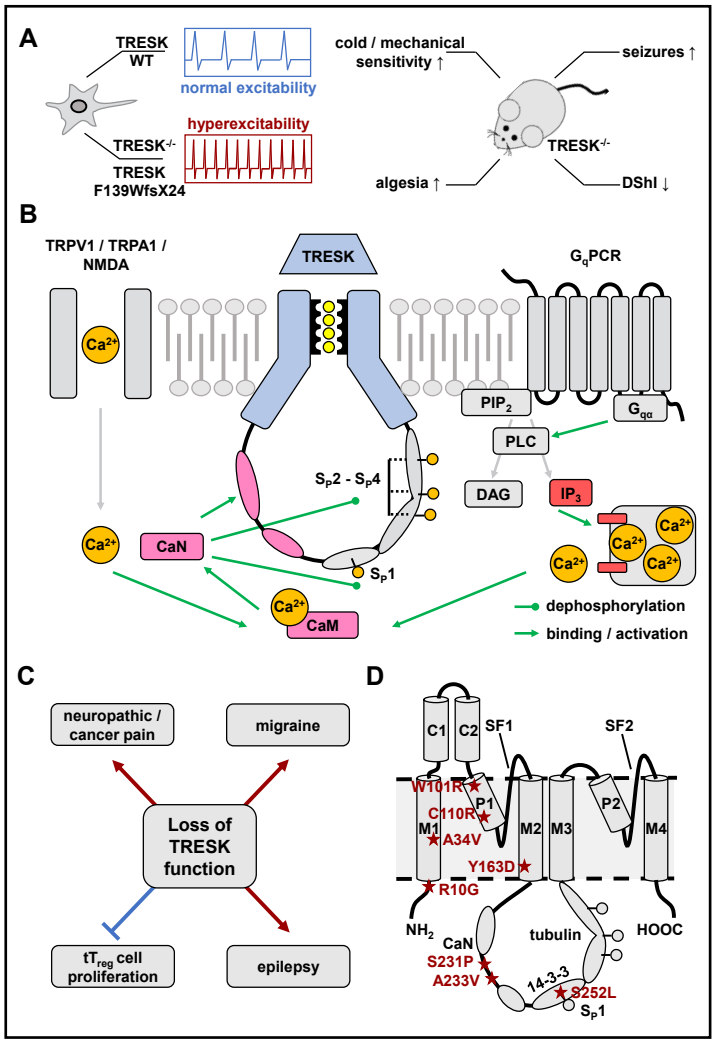


**Fig. 4.** A. Influence of (functional) TRESK knockout on neuronal firing and phenotype in mice. B. Intracellular mechanism of $Ca^{2+}$ / calmodulin (CaM) / calcineurin (CaN) induced channel activation. Cytosolic $Ca^{2+}$ concentration is influenced by $Ca^{2+}$ permeable ion channels (TRPV1, TRPA1, NDMA) as well as $G_q$-protein coupled receptors ($G_q$PCR), which induce $Ca^{2+}$ release from intracellular $Ca^{2+}$ reservoirs by activation of phospholipase C (PLC) subsequently converting $PIP_2$ into diacyl glycerol (DAG) and inositol-1,4,5-triphosphate ($IP_3$). C. Contribution of reduced TRESK function to physiological and pathophysiological processes. D. Localization of migraine-associated mutations at hTRESK.

Knockout studies also identified distinct subpopulations of neurons with high TRESK expression in TG mainly contributing to the observed differences [54, 55]. High rates of TRESK expression are found in isolectin B4 positive ($IB4^+$) nonpeptidergic small diameter neurons, that are likely to represent nociceptors of unmyelinated C-fibres [54]. Interestingly, these cells are also known to express the $Ca^{2+}$-permeable cation channels TRPV1 and TRPA1, which respond to noxious stimuli like natural pungent compounds (capsaicin, sanshool), $H^+$ or heat [58–60]. Recently, the direct interplay between TRPV1 and TRESK in primary sensory neurons was confirmed [52, 61]. TRESK channel activation can modify the $Ca^{2+}$ signal generated by capsaicin stimulation of isolated nociceptive neurons (Fig. 4B) [61]. Thus, TRESK acts like a brake for stimulatory TRPV1 effects on nociceptors [61]. Furthermore, pronounced TRESK expression was found in medium / large diameter calcitonin gene-related peptide ($CGRP^+$) or tropomyosin receptor kinase B ($TRKB^+$) positive neurons, which are part of the Aδ-nociceptor system [54]. In accordance with this, TRESK knockout mice show increased pain behavior and sensitivity to mechanical as well as cold stimuli while sensitivity to heat is nearly unaffected (Fig. 4A) [51, 54, 55, 57]. Although TRESK is not directly modulated by heat, TREK-2 displays pronounced cold sensitivity leading to absence of two major $K^+$ background components at lower temperatures in TRESK knockout mice [33, 49].

TRESK expression is reduced by nerve injuries [51]. *In vivo* axotomy in rats results in significantly reduced TRESK expression and subsequent hyperexcitability of DRG neurons 3 weeks after the procedure (Fig. 4A) [51]. Similar effects are observed by intrathecal siRNA application to control rats, that show decreased paw withdrawal threshold to mechanical stimuli [51]. In line with these results, overexpression of TRESK in nociceptive neurons significantly reduces the frequency of APs evoked by depolarizing currents or application of capsaicin [62, 63]. Thus, TRESK plays a key role in regulation of neuronal firing [62, 63].

Recent studies described similar mechanisms in the suprachiasmatic nucleus (SCN), an important structure for circadian rhythm of electrical activity, where TRESK channels serve as a critical opponent of glutamate-induced firing [56]. Stimulation of AMPA and NMDA receptors by glutamate causes an influx of $Ca^{2+}$ ions and subsequent depolarization / firing of neurons (Fig. 4B) [56]. Simultaneously, elevated cytosolic $Ca^{2+}$ concentrations activate TRESK channels via the calcineurin pathway ensuring repolarization and prevention of uncontrolled firing [56].

TRESK activation / overexpression does not only modulate the firing rate but also inhibits the release of substance P and the vasodilative peptide CGRP [61, 63–65]. Both peptides act as important neurotransmitters and are involved in pain transmission and in (neuro)inflammation [66, 67]. Thus, TRESK function might play an important role in distinct inflammatory processes as well, which is strengthened by many different studies [33, 68–71]. Endogenous mediators of inflammation like arachidonic acid are able to inhibit TRESK channels at low micromolar concentrations [25, 72]. However, histamine displays an exception, which can be explained by stimulation of the $G_q$-coupled $H_1$ receptor (Fig. 4B) [33, 69]. Activation of $G_q$-coupled receptors ($G_q$PCR) leads to increased $IP_3$ and diacyl glycerol (DAG) concentrations subsequently activating protein kinase C (PKC) and elevating intracellular $Ca^{2+}$ levels via the $IP_3$ receptor [26, 73]. In line with this, the antihistaminic drug loratadine displays a potent TRESK channel inhibitor [26, 73]. *In vivo* induced inflammation by injection of complete Freund's adjuvant leads to reduced expression of several $K_{2P}$ channels including TRESK on rat DRG neurons [62, 70]. On the other hand, overexpression of TRESK reduces not only the release of substance P and CGRP but also further inflammatory mediators like TNFα or IL1β [71]. Transgenic mice benefit from overexpressing TRESK in a model of spinal cord injury featuring accelerated paralysis recovery and reduced apoptotic signaling in the spinal cord [71].

Due to the fact, that TRESK is not only found in organs like thymus and spleen but also on distinct cell types like T-lymphocytes (Jurkat cells), a more general contribution to immunological processes was discussed [74–76]. Genetical and pharmacological evaluation using murine T-lymphocytes confirmed, that TRESK together with other $K_{2P}$ / $K_v$ channels is critically involved in osmo- and volume-regulation of the cell, which is essential for adaption of cell function under different immunological conditions [77, 78]. Very recently, TRESK channel involvement in regulatory T cell proliferation and maturation in the thymus ($tT_{reg}$) of mice and humans was confirmed, which are of critical role in immunosuppression and prevention of autoimmune diseases [68, 79]. Physiological $K^+$ ion conduction through TRESK channels is required for positive selection of $tT_{Reg}$ progenitor cells [68]. Pharmacological as well as genetic silencing of this $K^+$ conductance leads to reduced number of $tT_{Reg}$ cells elevating the risk of insufficient immunosuppression, while TRESK channel activation by cloxyquin and nitroxoline caused increased number of $tT_{Reg}$ cells [68]. In summary, the physiological role of TRESK in (neuro)inflammation and immunological processes is less understood than its role in pain sensation and transmission. However, these recent studies render TRESK an attractive target not only for analgesia but also immunomodulation.

### Diseases and pathophysiological conditions associated with TRESK

Although profound knowledge of TRESK contribution to distinct physiological processes was established, its contribution to pathophysiological conditions is less clear. Some evidence exists, that TRESK channels contribute to neuropathic (NP) and bone cancer-induced pain, which arise from lesions at the sensory nerve system caused by traumatic or inflammatory nerve damage (Fig. 4C) [80–82]. First association with NP was raised by the observed TRESK downregulation after *in vivo* axotomy [51]. Similar downregulation is also observed in the *in vivo* spared nerve injury (SNI) model, which mimics NP in rats [83]. SNI rats suffer from constant pain and hyperalgesia, which is associated with gliocyte / astrocyte activation and increased neuronal apoptosis [83, 84]. Although both phenomena are linked to TRESK downregulation, their assumed pathways differ. TRESK downregulation leads to upregulation of connexins Cx36 and Cx43, that contribute to gliocyte activation by formation of glia-neuron gap junctions subsequently inducing central sensitization and neuroinflammation [84, 85]. This is supported by elevated inflammatory cytokine levels as well as activation of mitogen-activated protein kinase (MAPK) pathway in SNI rats [84, 85]. On the other hand, neuronal apoptosis caused by TRESK silencing is associated with increased mRNA levels of Gm11874, that is upstream of ATP5i, a potential apoptosis gene mediating oxidative stress and DNA damage [86]. In line with these observations, adenoviral overexpression of TRESK in SNI rats partially inhibited gliocyte activation and neuronal apoptosis, thereby reducing severity of the pain and hyperalgesia [84–86]. Nevertheless, exact cellular as well as pathophysiological mechanisms of TRESK channel contribution to NP are poorly understood and need further investigations.

The presence of TRESK channels in TG as well as their physiological impact on neuronal firing and CGRP release quickly raised the question, if the channel contributes to the pathophysiology of migraine, which is a common recurrent headache disorder characterized by strong hemi cranial pain (Fig. 4C) [48]. About 30 % of pain attacks are accompanied by neurological disturbances (aura) like scintillating shapes, which are explained by uncontrolled neuronal firing followed by cortical spreading depression [48]. Indeed, genetic screening of patients suffering from migraine with aura identified a *KCNK18* frameshift mutation (F139WfsX24), that results in protein truncation eliminating typical TRESK channel current [48]. Analysis of TRESK F139WfsX24 in a human iPSC-derived nociceptor model reveals hyperexcitability compared to WT underlining the importance of TRESK acting as a brake upon depolarizing stimuli [87]. Interestingly, TRESK frameshift mutation inhibits not only TRESK but also TREK-1 and TREK-2 channel currents [11]. This is explained by the introduction of a second translational start codon introduced by the mutation leading to two different transcripts (MT1 / MT2) [11]. While MT1 inhibits TRESK WT, MT2 heterodimerizes with TREK-1 and TREK-2 subsequently inhibiting their physiological function as well, which might explain the pronounced hyperexcitability *in vitro* [11]. Over the years, more and more mutations were identified by genetical screening, that might be associated with migraine and aura (Fig. 4D) [11, 87–93]. Expression in *Xenopus laevis* followed by Two-electrode voltage clamp (TEVC) measurements identified C110R, A34V and W101R as loss-of-function mutations, while mutations S252L and Y163D did not alter basal but $Ca^{2+}$-stimulated activity of TRESK channels [90–92]. In contrast, mutations R10G, S231P and A233V were not significantly different to WT [90–92]. Despite the dominant loss of function observed in TEVC recordings, analysis of C110R in the human iPSC-derived nociceptor model did not reveal significant loss of TRESK current or hyperexcitability [87]. Similar observations were previously made by overexpression of TRESK C110R in primary mouse trigeminal neurons [94]. Together with the fact, that some mutations are not exclusively found in migraine patients, these observations suggest that TRESK might act as a risk factor rather than a direct cause of migraine [88, 95]. On the other hand, efficient reduction of spontaneous firing by the activator cloxyquin renders TRESK as a potential drug target for pharmacotherapy [87].

Since migraine shares genetic as well as pathophysiological features with other episodic neurological disorders, influence of TRESK function on epileptic seizures was examined as

well (Fig. 4C) [96]. Seizures result from neuronal hyperexcitability, which is associated with sustained neuronal depolarization and uncontrolled generation of APs [96]. *In vivo*, seizure episodes are self-limiting and followed by a period of suppressed cortical activity, that is induced by depolarization-induced shunting inhibition (DShI) [96]. DShI can suppress uncontrolled AP generation by membrane repolarization through activation of $K^+$ channels as well as inhibition of postsynaptic ionotropic receptors [96]. Electrophysiological analysis of hippocampal CA3 neurons from TRESK knockout mice confirmed a contribution of TRESK to the DShI, consistent with prolonged and severe seizure attacks observed in knockout mice as well as attenuated severity in mice overexpressing TRESK (Fig. 4A) [96].

Lastly, uprising evidence links TRESK channel function to inflammatory and immunological processes as described in the previous paragraph suggesting that TRESK might contribute to the development or severity of neurological autoimmune diseases like multiple sclerosis [68]. Especially its role in $tT_{reg}$ development and its response to (neuro) inflammatory conditions renders TRESK as an interesting target for immunomodulation [68]. However so far, a direct link between TRESK channel dysfunction and a distinct autoimmune disease was not found [97]. Further research is needed to examine the viability of TRESK as a pharmacological target for immune modulation [68, 97].

## TRESK channel activators

TRESK channel activity is modulated by a plethora of different compounds. For most of them, the exact mechanism is not established and an indirect modulation cannot be excluded due to the extensive possibilities for intracellular regulation of channel activity through the M2/M3 loop. Frequently used compounds for pharmacological TRESK channel modulation are summarized in Table 1 (activators), Table 2 (inhibitors) and Fig. 5. Wherever applicable, abbreviations used in Fig. 5 are mentioned in the text to facilitate the linkage between the description and the graphical illustration of the pharmacological mechanism.

Most $K_{2P}$ channels show enhanced conductance under the influence of volatile anesthetics (VA) [98]. As a consequence of elevated channel function, hyperpolarization of excitable neurons is induced contributing to the mechanism of general anesthesia [99]. Mutational studies at TASK-3 channels identified a possible binding site formed by residues of M2 and M3 at the intracellular site enabling stabilization of an open channel state [100]. It is assumed that binding to this site is linked to a common mechanism for volatile anesthetics (halogenated ethers) as well as sedative alcohols [100]. TRESK can be activated by typical volatile anesthetics like desflurane, halothane, isoflurane and sevoflurane leading to current potentiation up to 200 % [35, 98, 101]. The $EC_{50}$ values range from 162 µM (isoflurane) to 658 µM (desflurane, Table 1). For alcohols like 2-butanol, 2-pentanol and 2-hexanol only low current potentiation of 17 to 39 % can be observed at millimolar concentrations [102].

A more potent TRESK activator is cloxyquin (ClX), which was identified by $Tl^+$ flux screening [103]. Despite its simple molecular structure, cloxyquin achieved selectivity for TRESK over other $K_{2P}$ channels [32]. Mutational analysis indicates a direct modulation of the channel [32]. Single as well as double mutation of F156 and F364 at the mTRESK channel nearly abolish the agonistic effect [32]. However, exchange of these residues to alanine lead to strongly increased channel activity hampering the differentiation between cloxyquin and mutational effect [32]. Based on the cloxyquin scaffold several derivatives were synthesized and analyzed for their effect on mTRESK [104]. Interestingly, structural variation produced not only activators but also inhibitors [104]. Exchange of the quinoline to a naphthalene scaffold result in the new activator A2797 [104]. In comparison to cloxyquin, A2797 features comparable potency and efficiency at mTRESK, but reduced selectivity over mTREK-2 and mTASK-1 [104]. In addition, the structurally related antibiotic nitroxoline can activate hTRESK channels as well [68]. Although the agonistic effect of nitroxoline is lower than for cloxyquin, the evoked TRESK channel activation by nitroxoline is still able to induce $tT_{reg}$ cell maturation in the thymus [68].

**Table 1.** Summary of prominent TRESK channel activators and their $EC_{50}$ values [μM] at human (h), mouse (m) or rat (r) TRESK channels grouped by species. For each value the used assay as well as the reference is given. If no $EC_{50}$ was determined, percentage of activation (act.) is given together with the used concentration

| ligand | $EC_{50}$ / act. | conc. [μM] | spec. | assay | ref. |
|---|---|---|---|---|---|
| 2-butanol | 17 % act. | 16000 | h | TEVC (*Xenopus laevis*) | [102] |
| 2-hexanol | 37 % act. | 2000 | h | TEVC (*Xenopus laevis*) | [102] |
| 2-pentanol | 23 % act. | 4000 | h | TEVC (*Xenopus laevis*) | [102] |
| acetyl-β-methyl-choline | $EC_{50}$ | 0.65 | h | $Tl^+$ flux (HEK293) | [69] |
| arecoline | $EC_{50}$ | 2.7 | h | $Tl^+$ flux (HEK293) | [69] |
| BL-1249 | $EC_{50}$ | 6.0 | h | patch clamp (HEK293) | [101] |
| carbachol | $EC_{50}$ | 1.6 | h | $Tl^+$ flux (HEK293) | [69] |
| cloxyquin | $EC_{50}$ | 3.2 | h | patch clamp (U20S) | [103] |
| desflurane | $EC_{50}$ | 658 | h | TEVC (*Xenopus laevis*) | [98] |
| flufenamic acid | $EC_{50}$ | 474 | h | patch clamp (HEK293) | [101] |
| GI-530159 | $EC_{50}$ | 7.9 | h | $Tl^+$ flux (U-2 OS) | [106] |
| halothane | $EC_{50}$ | 300 | h | TEVC (*Xenopus laevis*) | [98] |
| isoflurane | $EC_{50}$ | 162 | h | TEVC (*Xenopus laevis*) | [98] |
| molecule 13 | $EC_{50}$ | 45 | h | patch clamp (HEK293) | [101] |
| molecule 15 | $EC_{50}$ | 18.8 | h | patch clamp (HEK293) | [101] |
| nitroxoline | 66 % act. | 300 | h | TEVC (*Xenopus laevis*) | [68] |
| OXA-22 | $EC_{50}$ | 0.06 | h | $Tl^+$ flux (HEK293) | [69] |
| oxotremorine | $EC_{50}$ | 0.24 | h | $Tl^+$ flux (HEK293) | [69] |
| PMA | $EC_{50}$ | 0.03 | h | $Tl^+$ flux (HEK293) | [69] |
| pranlukast | $EC_{50}$ | 2.5 | h | $Tl^+$ flux (U-2 OS) | [106] |
| sevoflurane | $EC_{50}$ | 224 | h | TEVC (*Xenopus laevis*) | [98] |
| spiperone | $EC_{50}$ | 3 | h | $Tl^+$ flux (HEK293) | [69] |
| A2797 | $EC_{50}$ | 54.4 | m | TEVC (*Xenopus laevis*) | [104] |
| cloxyquin | $EC_{50}$ | 26.4 | m | TEVC (*Xenopus laevis*) | [32] |
| isoflurane | $EC_{50}$ | 226 | m | TEVC (*Xenopus laevis*) | [35] |
| isoflurane | $EC_{50}$ | 346 | r | TEVC (*Xenopus laevis*) | [35] |

Another group of TRESK channel activators is derived from flufenamic acid (FFA), that is known for the stimulatory effect on TREK-1, TREK-2 and TRAAK channels [105]. At hTRESK channels, only weak current potentiation at high concentrations is observed [101]. Structural modifications led to molecule *13* and *15*, that have much higher potency and efficiency at hTRESK [101]. While efficiency of molecule *13* is comparable to cloxyquin, molecule *15* produced less pronounced current potentiation [101]. On the other hand, $EC_{50}$ of molecule *15* is reduced compared to molecule *13* [101]. Additionally, the flufenamic acid derivative BL-1249 exerts limited agonistic effects on hTRESK [101, 106]. However, BL-1249 is more potent at TREK-1 and TREK-2 channels than at TRESK [106]. Similar observations were made for the TREK-1 / TREK-2 channel agonist GI530159 that has residual activity at TRESK as well [106]. Interestingly, binding site of BL-1249 at TREK-2 is located at the M2/M4 interface partially overlapping with the corresponding site, that is assumed for binding of cloxyquin at TRESK channels [107]. It is further assumed, that binding of BL-1249 to TREK-1 / TREK-2 leads to repositioning of M4 subsequently stabilizing the conductive conformation of the SF [12].

As previously described, TRESK channel function is strongly modulated by regulatory proteins as well as intracellular $Ca^{2+}$ ions [30, 39, 40, 43, 45]. Therefore, indirect channel modulation by targeting these entities seems plausible. In $Tl^+$ assay, muscarinic receptor agonists like acetyl-β-methyl-choline, arecoline, carbachol, OXA-22 and oxotremorine achieved low to submicromolar $EC_{50}$ values at TRESK channels, that can be explained by the activation ($G_qA$) of $G_q$-coupled M3 receptors in HEK cells [69]. Interestingly, stimulation of TRESK by $G_q$-coupled receptors can be used as a readout for electrophysiological examination of $G_q$-coupled receptor activation in *Xenopus leavis* oocytes [108]. Furthermore, direct PKC activators like phorbol-12-myristate-13-acetate (PMA) activate TRESK channels at sub micromolar concentrations [106].

**Table 2.** Summary of TRESK channel inhibitors and their $IC_{50}$ values [μM] at human (h) or mouse (m) TRESK channels grouped by species. For each value the used assay as well as the reference is given. If no $IC_{50}$ was determined, percentage of inhibition (inh.) is given together with the used concentration

| ligand | $IC_{50}$ / inh. | conc. [μM] | spec. | assay | ref. |
|---|---|---|---|---|---|
| 6-gingerol | $IC_{50}$ | 155 | h | TEVC (*Xenopus laevis*) | [119] |
| 8-(3-chlorostyryl)caffeine | $IC_{50}$ | 22 | h | $Tl^+$ flux (HEK293) | [69] |
| arachidonic acid | $IC_{50}$ | 6.6 | h | patch clamp (L929) | [25] |
| aristolochic acid | $IC_{50}$ | 13 | h | patch clamp (tsA201) | [72] |
| bupivacaine | $IC_{50}$ | 80.4 | h | TEVC (*Xenopus laevis*) | [98] |
| calmidazolium | $IC_{50}$ | 27.9 | h | $Tl^+$ flux (HEK293) | [69] |
| capsaicin | $IC_{50}$ | 70.2 | h | TEVC (*Xenopus laevis*) | [119] |
| CEN-92 | 42 % inh. | 100 | h | patch clamp (tsA201) | [113] |
| chlorprocaine | $IC_{50}$ | 832 | h | TEVC (*Xenopus laevis*) | [98] |
| DCPIB | $IC_{50}$ | 0.14 | h | patch clamp (COS-7) | [115] |
| DOA | 55 % inh. | 20 | h | patch clamp (L929) | [25] |
| GW2974 | $IC_{50}$ | 26.6 | h | $Tl^+$ flux (HEK293) | [69] |
| JWH-015 | $IC_{50}$ | 5.47 | h | $Tl^+$ flux (HEK293) | [69] |
| K185 | $IC_{50}$ | 21.8 | h | $Tl^+$ flux (HEK293) | [69] |
| L162,313 | $IC_{50}$ | 11.5 | h | $Tl^+$ flux (HEK293) | [69] |
| L703,606 | $IC_{50}$ | 8.5 | h | $Tl^+$ flux (HEK293) | [69] |
| LA | 35 % inh. | 20 | h | patch clamp (L929) | [25] |
| lidocaine | $IC_{50}$ | 3400 | h | TEVC (*Xenopus laevis*) | [98] |
| loratadine | $IC_{50}$ | 0.69 | h | $Tl^+$ flux (HEK293) | [69] |
| mepivacaine | $IC_{50}$ | 1300 | h | TEVC (*Xenopus laevis*) | [98] |
| mevastatine | $IC_{50}$ | 9.42 | h | $Tl^+$ flux (HEK293) | [69] |
| MK-886 | $IC_{50}$ | 10.0 | h | $Tl^+$ flux (HEK293) | [69] |
| nicardipine | $IC_{50}$ | 21.9 | h | $Tl^+$ flux (HEK293) | [69] |
| nimodipine | $IC_{50}$ | 17.5 | h | $Tl^+$ flux (HEK293) | [69] |
| nitrendipine | $IC_{50}$ | 19.8 | h | $Tl^+$ flux (HEK293) | [69] |
| OA | 30 % inh. | 20 | h | patch clamp (L929) | [25] |
| octoclothepin | $IC_{50}$ | 7.23 | h | $Tl^+$ flux (HEK293) | [69] |
| oleyl CoA | 70 % inh. | 10 | h | patch clamp (*Xenopus laevis*) | [15] |
| oligomycin A | $IC_{50}$ | 3.71 | h | $Tl^+$ flux (HEK293) | [69] |
| PD98,059 | $IC_{50}$ | 14.6 | h | $Tl^+$ flux (HEK293) | [69] |
| piperine | $IC_{50}$ | 230.7 | h | TEVC (*Xenopus laevis*) | [119] |
| piperyline | $IC_{50}$ | 252 | h | TEVC (*Xenopus laevis*) | [120] |
| podophyllotoxin | $IC_{50}$ | 7.32 | h | $Tl^+$ flux (HEK293) | [69] |
| ropivacaine | $IC_{50}$ | 610 | h | TEVC (*Xenopus laevis*) | [98] |
| rottlerin | $IC_{50}$ | 16.2 | h | $Tl^+$ flux (HEK293) | [69] |
| sipatrigine | $IC_{50}$ | 34.0 | h | patch clamp (tsA201) | [113] |
| TButA | $IC_{50}$ | 7.0 | h | patch clamp (*Xenopus laevis*) | [109] |
| TEA | $IC_{50}$ | 800 | h | patch clamp (*Xenopus laevis*) | [109] |
| tetracaine | $IC_{50}$ | 496 | h | TEVC (*Xenopus laevis*) | [98] |
| tetrametrin | $IC_{50}$ | 10.7 | h | patch clamp (HEK293) | [126] |
| THepA | $IC_{50}$ | 0.5 | h | patch clamp (*Xenopus laevis*) | [109] |
| THexA | $IC_{50}$ | 0.5 | h | patch clamp (*Xenopus laevis*) | [109] |
| ToctA | $IC_{50}$ | 6 | h | patch clamp (*Xenopus laevis*) | [109] |
| TPenA | $IC_{50}$ | 0.3 | h | patch clamp (*Xenopus laevis*) | [109] |
| WIN55,212-2 | $IC_{50}$ | 17.8 | h | $Tl^+$ flux (HEK293) | [69] |
| YC-1 | $IC_{50}$ | 16.9 | h | $Tl^+$ flux (HEK293) | [69] |
| A2764 | $IC_{50}$ | 11.8 | m | TEVC (*Xenopus laevis*) | [104] |
| A2793 | $IC_{50}$ | 6.8 | m | TEVC (*Xenopus laevis*) | [104] |
| acetaminophen | $IC_{50}$ | 220 | m | Patch clamp (HEK293) | [111] |
| amitryptyline | $IC_{50}$ | 26 | m | patch clamp (HEK293) | [111] |
| $Ba^{2+}$ | 64 % inh. | 1000 | m | TEVC (*Xenopus laevis*) | [31] |
| bupropion | $IC_{50}$ | 160 | m | patch clamp (HEK293) | [111] |
| citalopram | $IC_{50}$ | 168.0 | m | patch clamp (HEK293) | [111] |
| cyclosporin A | 83 % inh. | 0.1 | m | TEVC (*Xenopus laevis*) | [30] |
| escitalopram | $IC_{50}$ | 49.0 | m | patch clamp (HEK293) | [111] |
| fluoxetine | $IC_{50}$ | 17.0 | m | patch clamp (HEK293) | [111] |
| $Hg^{2+}$ | 88 % inh. | 3 | m | patch clamp (COS-7) | [36] |
| ibuprofen | $IC_{50}$ | 889.0 | m | patch clamp (HEK293) | [111] |
| lamotrigine | $IC_{50}$ | 47 | m | patch clamp (COS-7) | [112] |
| mibefradil | $IC_{50}$ | 2.2 | m | TEVC (*Xenopus laevis*) | [36] |
| nabumetone | $IC_{50}$ | 557.0 | m | patch clamp (HEK293) | [111] |
| nifedipine | $IC_{50}$ | 63.8 | m | patch clamp (HEK293) | [116] |
| quinine | 82 % inh. | 100 | m | patch clamp (HEK293A) | [110] |
| sanshool | $IC_{50}$ | 50.2 | m | TEVC (*Xenopus laevis*) | [121] |
| tacrolimus (FK506) | 76 % inh. | 0.2 | m | TEVC (*Xenopus laevis*) | [30] |
| verapamil | $IC_{50}$ | 5.2 | m | patch clamp (HEK293) | [116] |
| $Zn^{2+}$ | $IC_{50}$ | 11.1 | m | TEVC (*Xenopus laevis*) | [35] |

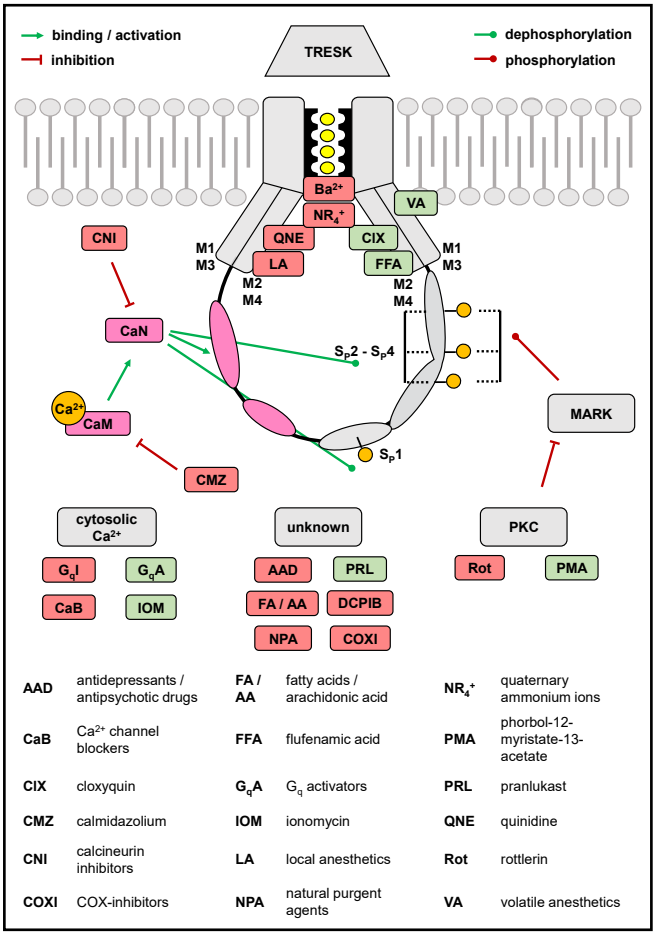


**Fig. 5.** Direct as well as indirect pharmacological modulation of TRESK by channel activators (green) and inhibitors (red). Abbreviations are summarized at figure bottom and correspond to abbreviations mentioned in the main text.

Contrary to this, the $CysLT_1$ antagonist pranlukast (PRL) activates TRESK although its target receptor is $G_q$-coupled [106]. Furthermore, pranlukast stimulates TREK-1, TREK-2 and TASK-3 [106]. Preliminary mutational analysis as well as usage of different TREK-2 isoforms failed to clarify if the agonistic effect is evoked by direct interaction with the channel or indirect stimulation via regulatory proteins [106].

### TRESK channel inhibitors

Compared to activators, much more compounds are known to inhibit TRESK channels in a direct or indirect manner (Table 2). Due to the similarity of the ion pore structure with other $K^+$ channels TRESK can be inhibited by quaternary ammonium ($NR_4^+$) as well as $Ba^{2+}$ ions [31, 109]. In contrast to TREK-1, hTRESK displays moderate sensitivity to tetraethylammonium (TEA) ions with an $IC_{50}$ value of 800 µM [109]. Potency is strongly increased for quaternary ammonium ions with enlarged alkyl chains up to seven C-atoms [109]. While tetrabutylammonium (TButA) achieves an $IC_{50}$ value in the low micromolar range, tetrapentyl- (TPenA), tetrahexyl- (THexA) and tetraheptylammonium ions share similar $IC_{50}$ values ranging from 0.3 - 0.5 µM [109]. For tetraoctylammonium (TOctA) ions the $IC_{50}$ value is increased to the level of TButA identifying the optimum alkyl chain length between five and seven C-atoms [109]. Although binding site determinations were not performed for hTRESK, similarities with the binding site analyzed in other $K_{2P}$ channels for quaternary ammonium ions can be assumed [109]. Mutational analyses at TREK-1 identified the binding site in the inner cavity directly neighbored to the SF leading to an obstruction

of the ion pathway [109]. This binding site is also in spatial proximity to the binding site of $Ba^{2+}$, that is formed by the S4-forming threonine of the SF present in TRESK channels [31]. Application of 1 mM $Ba^{2+}$ inhibit mTRESK channels by 64 % in TEVC measurements [31].

Another well-known $K^+$ channel blocker is quinine (QNE), that inhibits mTRESK by 82 % at 100 µM [110]. *In vitro* as well as *in silico* binding site analyses indicate, that the quinine binding site overlaps with the cloxyquin binding site [110]. Thus, this region at the inner cavity in proximity to the SF as well as the M2/M4 interface can be addressed by stimulatory as well as inhibitory compounds, that share a quinoline scaffold [32, 110]. Structural variation of cloxyquin led to the inhibitory compounds A2764 and A2793, that both possess an extended ether side chain in 8 position of the quinoline scaffold [104]. Although $IC_{50}$ values of both compounds are similar, their pharmacological profiles differ [104]. A2793 shows a strong state-dependent inhibition, that was amplified by previous stimulation of mTRESK with the $Ca^{2+}$ mobilizing agent ionomycin [104]. Further, A2793 also inhibits TASK-1 channels [104]. In comparison to this A2764 shows less state-dependent inhibition and higher selectivity rendering this compound as more suitable for selective TRESK channel inhibition [104].

The quinine binding site seems to be addressed by local anesthetics (LA) like lidocaine and bupivacaine as well [110]. Alanine mutation of mTRESK F156 / F364 largely abolished inhibition [110]. Later, mutational analysis of the corresponding residues in hTRESK (F145 / F352) led to similar findings [69]. Beside lidocaine and bupivacaine inhibitory activity at TRESK was also shown for chloroprocaine, mepivacaine, ropivacaine and tetracaine [98]. In TEVC measurements at hTRESK channels $IC_{50}$ values for local anesthetics range from 80.4 µM (bupivacaine) to 3.4 mM (lidocaine) [98]. More potent inhibition is achieved by the antihistaminic drug loratadine, which also loses its inhibitory activity at hTRESK F145A / F352A [69]. However, an additional indirect component through the inhibition of $G_q$-coupled $H_1$ receptors cannot be excluded.

Furthermore, some antidepressant and antipsychotic drugs (AAD) are known to inhibit TRESK [69, 111–113]. This includes amitriptyline, bupropion, citalopram, escitalopram, fluoxetine, lamotrigine and octoclothepine [69, 111–113]. $IC_{50}$ values determined by patch clamp recordings using mTRESK expressed in HEK293 range from 17 µM (fluoxetine) to 160 µM (bupropion) [111]. For octoclothepin a lower $IC_{50}$ value was determined at hTRESK using $Tl^+$ flux assay [69]. The mechanism of TRESK inhibition for these drugs is not known [69, 111–113]. However, binding site analysis of fluoxetine at TREK-2 showed, that fluoxetine binds to the M2/M4 interface and modulates the channel gating [114]. Direct channel inhibition is also assumed for sipatrigine and its derivative CEN-92 [113].

Recently, 4-[(2-butyl-6,7-dichloro-2-cyclopentyl-2,3-dihydro-1-oxo-1*H*-inden-5-yl)oxy] butanoic acid (DCPIB) was described as highly potent inhibitor of hTRESK [115]. DCPIB was previously described as a modulator of volume-regulated anion channels (VRACs) [115]. Interestingly, DCPIB modulates members of the $K_{2P}$ channel family differently [115]. While TRESK, TASK-1 and TASK-3 channels are inhibited, DCPIB is able to activate TREK-1 and TRAAK channels [115]. It is assumed, that $K_{2P}$ channel modulation by DCPIB is exerted by modulation of the lower S4 binding site modulating the conductance process through the SF differently for the distinct $K_{2P}$ channels [115].

Although a direct modulation of the channel cannot be excluded for the following compounds, an indirect inhibition seems to be more likely. Channel activity is reduced by $Ca^{2+}$ channel blockers (CaB) like dihydropyridines, verapamil and mibefradil [36, 69, 116]. While dihydropyridines like nicardipine, nifedipine, nimodipine and nitrendipine achieve $IC_{50}$ values in the mid micromolar range, verapamil and mibefradil seem to be slightly more potent [36, 69, 116].

Direct inhibition of calcineurin (CNI) or the upstream regulating protein calmodulin leads to TRESK inhibition as well [30, 69]. Cyclosporin A as well as tacrolimus (FK506) inhibit the ionomycin (IOM)-induced activation of TRESK at sub micromolar concentrations [30]. Remembering the physiological role of TRESK channels, this might also contribute to the calcineurin inhibitor–induced pain syndrome as well as strong headaches frequently

observed as side effects in immunosuppressant therapy with these drugs [117, 118]. The direct calmodulin inhibitor calmidazolium chloride (CMZ) is less potent but still able to inhibit hTRESK with an $IC_{50}$ of 27.9 µM [69]. Similar $IC_{50}$ values are achieved for the tubulin inhibitor podophyllotoxin (7.3 µM) and the PKC / calmodulin kinase inhibitor rottlerin (Rot) (16.2 µM) [69].

As previously described, TRESK is inhibited by endogenous fatty acids (FA) and arachidonic acid (AA) in the low micromolar range [15, 25]. This might also contribute to the inhibitory effect of cyclooxygenase inhibitors (COXI) on TRESK channels, which elevate the level of free arachidonic acid [111]. On the other hand, it is known that acetaminophen (paracetamol) and non-steroidal anti-inflammatory drugs (NSAIDs) can inhibit $K^+$ channels [111]. In case of acetaminophen, ibuprofen and nabumentone $IC_{50}$ values from 220 µM (acetaminophen) to 889 µM (ibuprofen) for mTRESK channel inhibition were evaluated by patch clamp [111].

Interestingly, many natural pungent agents (NPA) including capsaicin (chilli pepper), piperine and piperyline (black pepper), 6-gingerol (zingiber officinale) as well as sanshool (sichuan pepper) are known to inhibit TRESK [69, 119–121]. $IC_{50}$ values for these pungent compounds range from 50 µM (sanshool) to 252 µM (piperyline) [69, 119–121]. More potent with an $IC_{50}$ value of 13 µM is aristolochic acid, a common carcinogen found in *Aristolochiaceae* [72].

Finally, high throughput screening of research compounds and common channel modulators identified additional inhibitors including JWH-015, K185, L162,313, L703,606, PD98,059, WIN55,212-2, YC-1, MK-886, 8-(3-chlorostyryl)caffeine, mevastine, trametrin and GW2974 with $IC_{50}$ values ranging from 5.5 to 26.6 µM [69, 115]. Similar to most other TRESK channel modulators the mechanism of action for these compounds is not known and needs to be addressed by further examination.

## Conclusion

The TWIK-related spinal cord $K^+$ (TRESK) channel displays the most outstanding of the known $K_{2P}$ channels. The impressive number of regulatory pathways modulating channel activity let the channel contribute to many different cellular processes. Especially the contribution of TRESK to neuronal firing as well as the release inhibition of inflammatory mediators renders the channel a potential target for pharmacological intervention. In particular, agonistic compounds could serve as analgesics or antiepileptic drugs for treatment of migraine and epilepsy. Furthermore, the role of TRESK channel function in $tT_{reg}$ proliferation and maturation might offer a completely new strategy of pharmacological immunomodulation. On the other hand, the contribution of TRESK to other specific immunological processes or diseases like neuropathic pain as well as autoimmune diseases is insufficiently understood and needs further research. To boost the knowledge about TRESK contribution to different physiological and pathophysiological aspects, highly selective and potent TRESK channel activators and inhibitors are needed. Due to their relatively high specificity, cloxyquin and nitroxoline currently display the most suitable TRESK channel activators for *in vitro* / *in vivo* studies [32, 68]. In case of channel inhibitors, high TRESK channel specificity is achieved by the cloxyquin derivative A2764 and $Hg^{2+}$ ions [36, 104]. Furthermore, DCPIB might be a useful tool to distinguish between different $K_{2P}$ channels *in vitro* since its mechanism of action (activation / inhibition) is depending on the expressed $K_{2P}$ subtype [115]. However, most known TRESK channel activators and inhibitors show selectivity issues and / or low potency limiting the usage for further investigations. Therefore, further research as well as rational drug design is needed to uncover the therapeutic potential of TRESK channel modulation.

## Acknowledgements

We thank Prof. Dr. Bernhard Wünsch for carefully proofreading the manuscript.

*Author Contributions*
The manuscript was written by JAS with the help of MD and GS.

## Disclosure Statement

The authors declare that no conflict of interests exists.

## References

1 Kuang Q, Purhonen P, Hebert H: Structure of potassium channels. Cell Mol Life Sci 2015;72:3677–3693.
2 Wiedmann F, Frey N, Schmidt C: Two-Pore-Domain Potassium (K2P-) Channels: Cardiac Expression Patterns and Disease-Specific Remodelling Processes. Cells 2021;10:2914.
3 Miller C: An overview of the potassium channel family. Genome Biol 2000;1:Reviews0004.1–0004.5.
4 Trimmer JS: Subcellular localization of K+ channels in mammalian brain neurons: Remarkable precision in the midst of extraordinary complexity. Neuron 2015;85:238–256.
5 Taura J, Kircher DM, Gameiro-Ros I, Slesinger PA: Comparison of K+ Channel Families; in Gamper N, Wang K (eds): Pharmacology of Potassium Channels. Handb Exp Pharmacol 2021;267:1–49.
6 Lesage F, Guillemare E, Fink M, Duprat F, Lazdunski M, Romey G, Barhanin J: TWIK-1, a ubiquitous human weakly inward rectifying K+ channel with a novel structure. EMBO J 1996;15:1004–1111.
7 Turney TS, Li V, Brohawn SG: Structural Basis for pH-gating of the K+ channel TWIK1 at the selectivity filter. Nat Commun 2022;13:3232.
8 Lotshaw DP: Biophysical, pharmacological, and functional characteristics of cloned and native mammalian two-pore domain K+ channels. Cell Biochem Biophys 2007;47:209–256.
9 Blin S, Chatelain FC, Feliciangeli S, Kang D, Lesage F, Bichet D: Tandem pore domain halothane-inhibited K+channel subunits THIK1 and THIK2 assemble and form active channels. J Biol Chem 2014;289:28202–28212.
10 Berg AP, Talley EM, Manger JP, Bayliss DA: Motoneurons express heteromeric TWIK-related acid-sensitive K+ (TASK) channels containing TASK-1 (KCNK3) and TASK-3 (KCNK9) subunits. J Neurosci 2004;24:6693–6702.
11 Royal P, Andres-Bilbe A, Ávalos Prado P, Verkest C, Wdziekonski B, Schaub S, Baron A, Lesage F, Gasull X, Levitz J, Sandoz G: Migraine-Associated TRESK Mutations Increase Neuronal Excitability through Alternative Translation Initiation and Inhibition of TREK. Neuron 2019;101:232-245.
12 Pope L, Arrigoni C, Lou H, Bryant C, Gallardo-Godoy A, Renslo AR, Minor DL.: Protein and Chemical Determinants of BL-1249 Action and Selectivity for K 2P Channels. ACS Chem Neurosci. 2018;9:3153–3165.
13 Brohawn SG, del Mármol J, MacKinnon R: Crystal Structure of the Human K2P TRAAK, a Lipid- and Mechano-Sensitive K+ Ion Channel. Science 2012;335:436–441.
14 Miller AN, Long SB: Crystal Structure of the Human Two–Pore Domain Potassium Channel K2P1. Science 2012;335:432–436.
15 Riel EB, Jürs BC, Cordeiro S, Musinszki M, Schewe M, Baukrowitz T: The versatile regulation of K2P channels by polyanionic lipids of the phosphoinositide and fatty acid metabolism. J Gen Phys 2022;154:e202112989.
16 Niemeyer MI, Cid LP, Paulais M, Teulon J, Sepúlveda F: Phosphatidylinositol (4, 5)-bisphosphate dynamically regulates the K2P background K+ channel TASK-2. Sci Rep 2017;7:45407.
17 Enyedi P, Czirják G: Molecular background of leak K+ currents: Two-pore domain potassium channels. Physiol Rev 2010;90:559–605.
18 Natale AM, Deal PE, Minor DL: Structural Insights into the Mechanisms and Pharmacology of K2P Potassium Channels. J Mol Biol 2021;433:166995.

19 Zhang Q, Fu J, Zhang S, Guo P, Liu S, Shen J, Guo J, Yang H: 'C-type' closed state and gating mechanisms of K2P channels revealed by conformational changes of the TREK-1 channel. J Mol Cell Biol 2022;02120:1–20.
20 Proks P, Schewe M, Conrad LJ, Rao S, Rathje K, Rödström KEJ, Carpenter EP, Baukrowitz T, Tucker SJ: Norfluoxetine inhibits TREK-2 K2P channels by multiple mechanisms including state-independent effects on the selectivity filter gate. J Gen Phys 2021;153:1–13.
21 Lolicato M, Natale AM, Abderemane-Ali F, Crottès D, Capponi S, Duman R, Wagner A, Rosenberg JM, Grabe M, Minor DL: K2Pchannel C-type gating involves asymmetric selectivity filter order-disorder transitions. Sci Adv 2020;6:1–14.
22 Kopec W, Rothberg BS, de Groot BL: Molecular mechanism of a potassium channel gating through activation gate-selectivity filter coupling. Nat Commun 2019;10:1–15.
23 Rödström KEJ, Kiper AK, Zhang W, Rinné S, Pike ACW, Goldstein M, Conrad LJ, Delbeck M, Hahn MG, Meier H, Platzk M, Quigley A, Speedman D, Shrestha L, Mukhopadhyay SMM, Burgess-Brown NA, Tucker SJ, Müller T, Decher N, Carpenter EP: A lower X-gate in TASK channels traps inhibitors within the vestibule. Nature 2020;582:443–447.
24 Kamuene JM, Xu Y, Plant LD: The Pharmacology of Two-Pore Domain Potassium Channels; in Gamper N, Wang K (eds): Pharmacology of Potassium Channels. Handb Exp Pharmacol 2021;267:417–443.
25 Sano Y, Inamura K, Miyake A, Mochizuki S, Kitada C, Yokoi H, Nozawa K, Okada H, Matsushime H, Furuichi K: A novel two-pore domain K+ channel, TRESK, is localized in the spinal cord. J Biol Chem 2003;278:27406–27412.
26 Czirják G, Enyedi P: Targeting of calcineurin to an NFAT-like docking site is required for the calcium-dependent activation of the background K+ channel, TRESK. J Biol Chem 2006;281:14677–14682.
27 Kang D, Mariash E, Kim D: Functional expression of TRESK-2, a new member of the tandem-pore K + channel family. J Biol Chem 2004;279:28063–28070.
28 Rahm AK, Wiedmann F, Gierten J, Schmidt C, Schweizer PA, Becker R, Katus HA, Thomas D: Functional characterization of zebrafish K2P18.1 (TRESK) two-pore-domain K+ channels. Naunyn Schmiedebergs Arch Pharmacol 2014;387:291–300.
29 Callejo G, Giblin JP, Gasull X: Modulation of TRESK Background K+ Channel by Membrane Stretch. PLoS One 2013;8:1–12.
30 Czirják G, Tóth ZE, Enyedi P: The Two-pore Domain K+ Channel, TRESK, Is Activated by the Cytoplasmic Calcium Signal through Calcineurin. J Biol Chem 2004;279:18550–18558.
31 Lengyel M, Czirják G, Enyedi P: TRESK background potassium channel is not gated at the helix bundle crossing near the cytoplasmic end of the pore. PLoS One 2018;13:1–16.
32 Lengyel M, Dobolyi A, Czirják G, Enyedi P: Selective and state-dependent activation of TRESK (K2P 18.1) background potassium channel by cloxyquin. Br J Pharmacol 2017;174:2102–2113.
33 Dobler T, Springauf A, Tovornik S, Weber M, Schmitt A, Sedlmeier R, Wischmeyer E, Döring F: TRESK two-pore-domain K+ channels constitute a significant component of background potassium currents in murine dorsal root ganglion neurones. J Physiol 2007;585:867–879.
34 Rajan S, Wischmeyer E, Liu GX, Preisig-Müller R, Daut J, Karschin A, Derst C.: TASK-3, a novel tandem pore domain acid-sensitive K+ channel. An extracellular histidine as pH sensor. J Biol Chem 2000;275:16650–16657.
35 Keshavaprasad B, Liu C, Au JD, Kindler CH, Cotten JF, Yost CS: Species-specific differences in response to anesthetics and other modulators by the K2P channel TRESK. Anesth Analg 2005;101:1042–1049.
36 Czirják G, Enyedi P: Zinc and mercuric ions distinguish TRESK from the other two-pore-domain K+ channels. Mol Pharmacol 2006;69:1024–1032.
37 Egenberger B, Polleichtner G, Wischmeyer E, Döring F: N-linked glycosylation determines cell surface expression of two-pore-domain K+ channel TRESK. Biochem Biophys Res Commun 2010;391:1262–1267.
38 Giblin JP, Etayo I, Castellanos A, Andres-Bilbe A, Gasull X: Anionic Phospholipids Bind to and Modulate the Activity of Human TRESK Background K + Channel. Mol Neurobiol 2019;56:2524–2541.
39 Czirják G, Enyedi P: The LQLP calcineurin docking site is a major determinant of the calcium-dependent activation of human TRESK background K+ channel. J Biol Chem 2014;289:29506–29518.
40 Czirják G, Enyedi P: TRESK background K+ channel is inhibited by phosphorylation via two distinct pathways. J Biol Chem 2010;285:14549–14557.
41 Czirják G, Vuity D, Enyedi P: Phosphorylation-dependent binding of 14-3-3 proteins controls TRESK regulation. J Biol Chem 2008;283:15672–15680.

42 Chaudhri M, Scarabel M, Aitken A: Mammalian and yeast 14-3-3 isoforms form distinct patterns of dimers *in vivo*. Biochem Biophys Res Commun 2003;300:679–685.
43 Enyedi P, Veres I, Braun G, Czirják G: Tubulin binds to the cytoplasmic loop of TRESK background K+ channel *in vitro*. PLoS One 2014;9:e97854.
44 Matenia D, Mandelkow E-M: The tau of MARK: a polarized view of the cytoskeleton. Trends Biochem Sci 2009;34:332–342.
45 Braun G, Nemcsics B, Enyedi P, Czirják G: Tresk background K+ channel is inhibited by PAR-1/MARK microtubule affinity-regulating kinases in Xenopus oocytes. PLoS One 2011;6:1–10.
46 Rahm AK, Gierten J, Kisselbach J, Staudacher I, Staudacher K, Schweizer PA, Becker R, Katus HA, Thomas D: PKC-dependent activation of human K 2P18.1 K + channels. Br J Pharmacol 2012;166:764–773.
47 Pergel E, Lengyel M, Enyedi P, Czirják G: TRESK (K2P18.1) background potassium channel is activated by novel-type protein kinase C via dephosphorylation. Mol Pharmacol 2019;95:661–672.
48 Lafrenière RG, Cader MZ, Poulin JF, Andres-Enguix I, Simoneau M, Gupta N, Boisvert K, Lafrenière F, McLaughlan S, Dube MP, Marcinkiewicz MM, Ramagopalan S, Ansorge O, Brais B, Sequeiros J, Pereira-Monteiro JM, Griffiths LR, Tucker SJ, Ebers G, Rouleau GA: A dominant-negative mutation in the TRESK potassium channel is linked to familial migraine with aura. Nat Med 2010;16:1157–1160.
49 Kang D, Kim D: TREK-2 (K2P10.1) and TRESK (K2P18.1) are major background K+ channels in dorsal root ganglion neurons. Am J Physiol Cell Physiol 2006;291:138–146.
50 Yoo SH, Liu J, Sabbadini M, Au P, Xie G xi, Yost CS: Regional expression of the anesthetic-activated potassium channel TRESK in the rat nervous system. Neurosci Lett 2009;465:79–84.
51 Tulleuda A, Cokic B, Callejo G, Saiani B, Serra J, Gasull X: TRESK channel contribution to nociceptive sensory neurons excitability: Modulation by nerve injury. Mol Pain 2011;7:30.
52 Kollert S, Dombert B, Döring F, Wischmeyer E: Activation of TRESK channels by the inflammatory mediator lysophosphatidic acid balances nociceptive signalling. Sci Rep 2015;5:1–14.
53 Manteniotis S, Lehmann R, Flegel C, Vogel F, Hofreuter A, Schreiner BSP, Altmüller J, Becker C, Schöbel N, Hatt H, Gisselmann G: Comprehensive RNA-Seq Expression Analysis of Sensory Ganglia with a Focus on Ion Channels and GPCRs in Trigeminal Ganglia. PLoS One 2013;8:e79523.
54 Weir GA, Pettingill P, Wu Y, Duggal G, Ilie AS, Akerman CJ, Cader MZ: The role of TRESK in discrete sensory neuron populations and somatosensory processing. Front Mol Neurosci 2019;12:1–11.
55 Castellanos A, Pujol-Coma A, Andres-Bilbe A, Negm A, Callejo G, Soto D, Noel J, Comes N, Gasull X: TRESK background K+ channel deletion selectively uncovers enhanced mechanical and cold sensitivity. J Physiol 2020;598:1017–1038.
56 Lalic T, Steponenaite A, Wei L, Vasudevan SR, Mathie A, Peirson SN, Lall GS, Cader MZ: TRESK is a key regulator of nocturnal suprachiasmatic nucleus dynamics and light adaptive responses. Nat Commun 2020;11:1–11.
57 Guo Z, Qiu CS, Jiang X, Zhang J, Li F, Liu Q, Dhaka A, Cao Y-Q: TRESK K+ channel activity regulates trigeminal nociception and headache. eNeuro 2019;6:ENEURO.0236-19.2019.
58 Huang D, Li S, Dhaka A, Story GM, Cao Y-Q: Expression of the transient receptor potential channels TRPV1, TRPA1 and TRPM8 in mouse trigeminal primary afferent neurons innervating the dura. Mol Pain 2012;66:1-19.
59 Koo JY, Jang Y, Cho H, Lee CH, Jang KH, Chang YH, Shin J, Oh U: Hydroxy-α-sanshool activates TRPV1 and TRPA1 in sensory neurons. European Journal of Neuroscience 2007;26:1139–1147.
60 Breese NM, George AC, Pauers LE, Stucky CL: Peripheral inflammation selectively increases TRPV1 function in IB4-positive sensory neurons from adult mouse. Pain 2005;115:37–49.
61 Lengyel M, Hajdu D, Dobolyi A, Rosta J, Czirják G, Dux M, Enyedi P: TRESK background potassium channel modifies the TRPV1-mediated nociceptor excitability in sensory neurons. Cephalalgia 2021;41:827–838.
62 Guo Z, Cao YQ: Over-expression of TRESK K+ channels reduces the excitability of trigeminal ganglion nociceptors. PLoS One 2014;9:1–13.
63 Zhou J, Yao SL, Yang CX, Zhong JY, Wang HB, Zhang Y: TRESK gene recombinant adenovirus vector inhibits capsaicin-mediated substance P release from cultured rat dorsal root ganglion neurons. Mol Med Rep 2012;5:1049–1052.
64 Louis-Gray K, Tupal S, Premkumar LS: TRPV1: A Common Denominator Mediating Antinociceptive and Antiemetic Effects of Cannabinoids. Int J Mol Sci 2022;23:10016.

65 Nakato R, Manabe N, Hanayama K, Kusunoki H, Hata J, Haruma K: Diagnosis and treatments for oropharyngeal dysphagia: effects of capsaicin evaluated by newly developed ultrasonographic method. J Smooth Muscle Res 2020;56:46–57.
66 Balcziak LK, Russo AF: Dural Immune Cells, CGRP, and Migraine. Front Neurol 2022;13:874193.
67 Muñoz M, Coveñas R: Involvement of substance P and the NK-1 receptor in human pathology. Amino Acids 2014;46:1727–1750.
68 Ruck T, Bock S, Pfeuffer S, Schroeter CB, Cengiz D, Marciniak P, Lindner M, Herrmann A, Liebmann M, Kovac S, Gola L, Rolfes L, Pawlitzki M, Opel N, Hahn T, Dannlowski U, Pap T, Luessi F, Schreiber JA, Wünsch B, et al.: K2P18.1 translates T cell receptor signals into thymic regulatory T cell development. Cell Res 2022;32:72–88.
69 Bruner JK, Zou B, Zhang H, Zhang Y, Schmidt K, Li M: Identification of novel small molecule modulators of K2P18.1 two-pore potassium channel. Eur J Pharmacol 2014;740:603–610.
70 Marsh B, Acosta C, Djouhri L, Lawson SN: Leak K + channel mRNAs in dorsal root ganglia: Relation to inflammation and spontaneous pain behaviour. Molecular and Cellular Neuroscience. 2012;49:375–386.
71 Kim GT, Siregar AS, Kim EJ, Lee ES, Nyiramana MM, Woo MS, Hah Y-S, Han J, Kang D: Upregulation of tresk channels contributes to motor and sensory recovery after spinal cord injury. Int J Mol Sci 2020;21:1–15.
72 Veale EL, Mathie A: Aristolochic acid, a plant extract used in the treatment of pain and linked to Balkan endemic nephropathy, is a regulator of K2P channels. Br J Pharmacol 2016;173:1639–1652.
73 Falkenburger BH, Dickson EJ, Hille B: Quantitative properties and receptor reserve of the DAG and PKC branch of Gq-coupled receptor signaling. J Gen Physiol 2013;141:537–555.
74 Han J, Kang D: TRESK channel as a potential target to treat T-cell mediated immune dysfunction. Biochem Biophys Res Commun 2009;390:1102–1105.
75 Pottosin II, Bonales-Alatorre E, Valencia-Cruz G, Mendoza-Magaña ML, Dobrovinskaya OR: TRESK-like potassium channels in leukemic T cells. Pflugers Arch 2008;456:1037–1048.
76 Sánchez-Miguel DS, García-Dolores F, Rosa Flores-Márquez M, Delgado-Enciso I, Pottosin I, Dobrovinskaya O: TRESK potassium channel in human T lymphoblasts. Biochem Biophys Res Commun 2013;434:273–279.
77 Bobak N, Bittner S, Andronic J, Hartmann S, Mühlpfordt F, Schneider-Hohendorf T, Wolf K, Schmelter C, Göbel K, Meuth P, Zimmermann H, Döring F, Wischmeyer E, Budde T, Wiendl H, Meuth SG, Sukhorukov VL: Volume regulation of murine T lymphocytes relies on voltage-dependent and two-pore domain potassium channels. Biochim Biophys Acta Biomembr 2011;1808:2036–2044.
78 Brown CC, Gottschalk RA: Volume control: Turning the dial on regulatory T cells. Cell 2021;184:3847–3849.
79 Bettelli E, Carrier Y, Gao W, Korn T, Strom TB, Oukka M, Weiner HL, Kuchroo VK: Reciprocal developmental pathways for the generation of pathogenic effector TH17 and regulatory T cells. Nature 2006;441:235–238.
80 Shkodra M, Caraceni A: Treatment of Neuropathic Pain Directly Due to Cancer: An Update. Cancers (Basel) 2022;14:1992.
81 Liu JP, Jing HB, Xi K, Zhang ZX, Jin ZR, Cai SQ, Tian Y, Cai J, Xing G-G: Contribution of TRESK two-pore domain potassium channel to bone cancer-induced spontaneous pain and evoked cutaneous pain in rats. Mol Pain 2021;17:1-18.
82 Yang Y, Li S, Jin ZR, Jing HB, Zhao HY, Liu BH, Liang YJ, Cai J, Wan Y, Xing G-G: Decreased abundance of TRESK two-pore domain potassium channels in sensory neurons underlies the pain associated with bone metastasis. Sci Signal 2018;11:eaao5150.
83 Zhou J, Yang CX, Zhong JY, Wang HB: Intrathecal TRESK gene recombinant adenovirus attenuates spared nerve injury-induced neuropathic pain in rats. Neuroreport 2013;24:131–136.
84 Zhou J, Lin W, Chen H, Fan Y, Yang C: TRESK contributes to pain threshold changes by mediating apoptosis via MAPK pathway in the spinal cord. Neuroscience 2016;339:622–633.
85 Zhou J, Chen H, Yang C, Zhong J, He W, Xiong Q: Reversal of TRESK Downregulation Alleviates Neuropathic Pain by Inhibiting Activation of Gliocytes in the Spinal Cord. Neurochem Res 2017;42:1288–1298.
86 Liu P, Cheng Y, Xu H, Huang H, Tang S, Song F, Zhou J: TRESK Regulates Gm11874 to Induce Apoptosis of Spinal Cord Neurons via ATP5i Mediated Oxidative Stress and DNA Damage. Neurochem Res 2021;46:1970–1980.
87 Pettingill P, Weir GA, Wei T, Wu Y, Flower G, Lalic T, Handel A, Duggal G, Chintawar S, Cheung J, Arunasalam K, Couper E, Haupt LM, Griffiths LR, Bassett A, Cowley SA, Cader MZ: A causal role for TRESK loss of function in migraine mechanisms. Brain 2019;142:3852–3867.

88 Gada K, Plant LD: Two-pore domain potassium channels: emerging targets for novel analgesic drugs: IUPHAR Review 26. Br J Pharmacol 2019;176:256–266.
89 Rainero I, Rubino E, Gallone S, Zavarise P, Carli D, Boschi S, Fenoglio P, Savi L, Gentile S, Benna P, Pinessi L, Dalla Volta G: KCNK18 (TRESK) genetic variants in Italian patients with migraine. Headache 2014;54:1515–1522.
90 Andres-Enguix I, Shang L, Stansfeld PJ, Morahan JM, Sansom MSP, Lafrenière RG, Roy B, Griffiths LR, Rouleau GA, Ebers GC, Cader ZM, Tucker SJ: Functional analysis of missense variants in the TRESK (KCNK18) K + channel. Sci Rep 2012;2:1–7.
91 Imbrici P, Nematian-Ardestani E, Hasan S, Pessia M, Tucker SJ, D'Adamo MC: Altered functional properties of a missense variant in the TRESK K+ channel (KCNK18) associated with migraine and intellectual disability. Pflugers Arch 2020;472:923–930.
92 Pavinato L, Nematian-Ardestani E, Zonta A, de Rubeis S, Buxbaum J, Mancini C, Bruselles A, Tartaglia M, Pessia M, Tucker SJ, D'Adamo MC, Brusco A: Kcnk18 biallelic variants associated with intellectual disability and neurodevelopmental disorders alter tresk channel activity. Int J Mol Sci 2021;22:6064.
93 Han JY, Jang JH, Park J, Lee IG: Targeted next-generation sequencing of Korean patients with developmental delay and/or intellectual disability. Front Pediatr 2018;6:1–9.
94 Guo Z, Liu P, Ren F, Cao YQ: Nonmigraine-associated TRESK K+ channel variant c110r does not increase the excitability of trigeminal ganglion neurons. J Neurophysiol 2014;112:568–579.
95 Markel KA, Curtis D: Study of variants in genes implicated in rare familial migraine syndromes and their association with migraine in 200,000 exome-sequenced UK Biobank participants. Ann Hum Genet 2022;86:353-360.
96 Huang W, Ke Y, Zhu J, Liu S, Cong J, Ye H, Guo Y, Wang K, Zhang Z, Meng W, Gao T-M, Luhmann HJ, Kilb W, Chen R: TRESK channel contributes to depolarization-induced shunting inhibition and modulates epileptic seizures. Cell Rep 2021;36:109404.
97 Huntemann N, Bittner S, Bock S, Meuth SG, Ruck T: Mini-Review: Two Brothers in Crime – The Interplay of TRESK and TREK in Human Diseases. Neurosci Lett 2022;769:136376.
98 Liu C, Au JD, Zou HL, Cotten JF, Yost CS: Potent activation of the human tandem pore domain K channel TRESK with clinical concentrations of volatile anesthetics. Anesth Analg 2004;99:1715–1722.
99 Zhou W, Guan Z: Ion Channels in Anesthesia. Adv Exp Med Biol 2021;1349:401–413.
100 Luethy A, Boghosian JD, Srikantha R, Cotten JF: Halogenated ether, alcohol, and alkane anesthetics activate TASK-3 tandem pore potassium channels likely through a common mechanism. Mol Pharmacol 2017;91:620–629.
101 Monteillier A, Loucif A, Omoto K, Stevens EB, Vicente SL, Saintot PP, Cao L, Pryde DC: Investigation of the structure activity relationship of flufenamic acid derivatives at the human TRESK channel K2P18.1. Bioorg Med Chem Lett 2016;26:4919–4924.
102 Brosnan R, Gong D, Cotten J, Keshavaprasad B, Yost CS, Eger EI, Sonner JM.: Chirality in anesthesia II: Stereoselective modulation of ion channel function by secondary alcohol enantiomers. Anesth Analg 2006;103:86–91.
103 Wright PD, Weir G, Cartland J, Tickle D, Kettleborough C, Cader MZ, Jerman J: Cloxyquin (5-chloroquinolin-8-ol) is an activator of the two-pore domain potassium channel TRESK. Biochem Biophys Res Commun 2013;441:463–468.
104 Lengyel M, Erdélyi F, Pergel E, Bálint-Polonka Á, Dobolyi A, Bozsaki P, Dux M, Kiraly K, Hegedus T, Czirjak G, Matyus P, Enyedi P: Chemically modified derivatives of the activator compound cloxyquin exert inhibitory effect on TRESK (K2P18.1) background potassium channel. Mol Pharmacol 2019;95:652–660.
105 Takahira M, Mayumi AE, Norimasa S, Ae S, Sugiyama K: Fenamates and diltiazem modulate lipid-sensitive mechano-gated 2P domain K + channels. Eur J Physiol 2005;451:474-478.
106 Wright PD, McCoull D, Walsh Y, Large JM, Hadrys BW, Gaurilcikaite E, Byrom L, Veale EL, Jerman J, Mathie A: Pranlukast is a novel small molecule activator of the two-pore domain potassium channel TREK2. Biochem Biophys Res Commun 2019;520:35–40.
107 Schewe M, Sun H, Mert Ü, Mackenzie A, Pike ACW, Schulz F, Constantin C, Vowinkel KS, Conrad LJ, Kiper AK, Gonzalez W, Musinszki M, Tegtmeier M, Pryde DC, Belabed H, Nazare M, de Groot BL, Decher N, Fakler B, Carpenter EP, et al.: A pharmacological master key mechanism that unlocks the selectivity filter gate in K channels. Science 2019;363:875–880.

108 Subramanian H, Döring F, Kollert S, Rukoyatkina N, Sturm J, Gambaryan S, Stellzig-Eisenhauer A, Meyer-Marcotty P, Eigenthaler M, Wischmeyer E: PTH1R mutants found in patients with primary failure of tooth eruption disrupt G-protein signaling. PLoS One 2016;11:1–16.
109 Piechotta PL, Rapedius M, Stansfeld PJ, Bollepalli MK, Erhlich G, Andres-Enguix I, Fritzenschaft H, Decher N, Sansom MSP, Tucker SJ, Baukrowitz, T: The pore structure and gating mechanism of K2P channels. EMBO J 2011;30:3607–3619.
110 Kim S, Lee Y, Tak HM, Park HJ, Sohn YS, Hwang S, Han J, Kang D, Lee KW: Identification of blocker binding site in mouse TRESK by molecular modeling and mutational studies. Biochim Biophys Acta Biomembr 2013;1828:1131–1142.
111 Park H, Kim EJ, Han J, Han J, Kang D: Effects of analgesics and antidepressants on TREK-2 and TRESK currents. Korean J Physiol Pharmacol 2016;20:379–385.
112 Kang D, Kim GT, Kim EJ, La JH, Lee JS, Lee ES, Park JY, Hong SG, Han J: Lamotrigine inhibits TRESK regulated by G-protein coupled receptor agonists. Biochem Biophys Res Commun 2008;367:609–615.
113 Walsh Y, Leach M, Veale EL, Mathie A: Block of TREK and TRESK K2P channels by lamotrigine and two derivatives sipatrigine and CEN-092. Biochem Biophys Rep 2021;26:101021.
114 Dong YY, Pike ACW, Mackenzie A, McClenaghan C, Aryal P, Dong L, Quigley A, Grieben M, Goubin S, Mukhopadhyay S, Ruda GF, Clausen MV, Cao L, Brennan PE, Burgess-Brown NA, Sansom MSP, Tucker SJ, Carpenter EP: K2P channel gating mechanisms revealed by structures of TREK-2 and a complex with Prozac. Science 2015;347:1256–1259.
115 Lv J, Liang Y, Zhang S, Lan Q, Xu Z, Wu X, Kang L, Ren J, Cao Y, Wu T, Lin KL, Yung KKL, Cao X, Pang J, Zhou P: DCPIB, an Inhibitor of Volume-Regulated Anion Channels, Distinctly Modulates K2P Channels. ACS Chem Neurosci 2019;10:2786–2793.
116 Park H, Kim EJ, Ryu JH, Lee DK, Hong SG, Han J, Han J, Kang D: Verapamil inhibits TRESK (K2p18.1) current in trigeminal ganglion neurons independently of the blockade of Ca2+ influx. Int J Mol Sci 2018;19:1–13.
117 Huang Y, Chen SR, Pan HL: Calcineurin Regulates Synaptic Plasticity and Nociceptive Transmissionat the Spinal Cord Level. Neuroscientist 2022;28:628-638.
118 Ferrari U, Empl M, Kim KS, Sostak P, Förderreuther S, Straube A: Calcineurin inhibitor-induced headache: Clinical characteristics and possible mechanisms. Headache 2005;45:211–214.
119 Beltrán LR, Dawid C, Beltrán M, Gisselmann G, Degenhardt K, Mathie K, Hofmann T, Hatt H: The pungent substances piperine, capsaicin, 6-gingerol and polygodial inhibit the human two-pore domain potassium channels TASK-1, TASK-3 and TRESK. Front Pharmacol 2013;4:1–11.
120 Beltrán LR, Dawid C, Beltrán M, Levermann J, Titt S, Thomas S, Pürschel V, Satalik M, Gisselmann G, Hofmann T, Hatt H: The effect of pungent and tingling compounds from Piper nigrum L. on background K+ currents. Front Pharmacol 2017;8:1–14.
121 Bautista DM, Sigal YM, Milstein AD, Garrison JL, Zorn JA, Tsuruda PR, Nicoll RA, Julius D: Pungent agents from Szechuan peppers excite sensory neurons by inhibiting two-pore potassium channels. Nat Neurosci 2008;11:772–779.
122 Kumar S, Stecher G, Li M, Knyaz C, Tamura K: MEGA X: Molecular Evolutionary Genetics Analysis across Computing Platforms. Mol Biol Evol 2018;35:1547–1549.
123 Jumper J, Evans R, Pritzel A, Green T, Figurnov M, Ronneberger O, Tunyasuvunakool K, Bates R, Žídek A, Potapenko A, Bridgland A, Meyer C, Kohl SAA, Ballard AJ, Cowie A, Romera-Paredes B, Nikolov S, Jain R, Adler J, Back T, et al.: Highly accurate protein structure prediction with AlphaFold. Nature 2021;596:583–589.
124 Varadi M, Anyango S, Deshpande M, Nair S, Natassia C, Yordanova G, Yuan D, Stroe O, Wood G, Laydon A, Zidek A, Green T, Tunyasuvunakool K, Petersen S, Jumper J, Clancy E, Green R, Vora A, Lutfi M, Figurnov M, et al.: AlphaFold Protein Structure Database: massively expanding the structural coverage of protein-sequence space with high-accuracy models. Nucleic Acids Res 2022;50:D439–D444.
125 Krieger E, Vriend G: YASARA View—molecular graphics for all devices—from smartphones to workstations. Bioinformatics. 2014;30:2981–2982.
126 Castellanos A, Andres A, Bernal L, Callejo G, Comes N, Gual A, Giblin JP, Roza C, Gasull X: Pyrethroids inhibit K2P channels and activate sensory neurons: Basis of insecticide-induced paraesthesias. Pain 2018;159:92–105.